Copyright Warning & Restrictions

The copyright law of the United States (Title 17, United States Code) governs the making of photocopies or other reproductions of copyrighted material.

Under certain conditions specified in the law, libraries and archives are authorized to furnish a photocopy or other reproduction. One of these specified conditions is that the photocopy or reproduction is not to be "used for any purpose other than private study, scholarship, or research." If a, user makes a request for, or later uses, a photocopy or reproduction for purposes in excess of "fair use" that user may be liable for copyright infringement,

This institution reserves the right to refuse to accept a copying order if, in its judgment, fulfillment of the order would involve violation of copyright law.

Please Note: The author retains the copyright while the New Jersey Institute of Technology reserves the right to distribute this thesis or dissertation

Printing note: If you do not wish to print this page, then select "Pages from: first page # to: last page #" on the print dialog screen

ABSTRACT

NUMERICAL SIMULATION AND INITIAL EXPERIMENTS FOR IDENTIFICATION OF INSECTS USING A CW LIDAR SYSTEM

by
Christo Videlov

Mosquitos are the most common vector of disease in the world, causing millions of deaths a year. While curing the diseases they cause is one approach to this problem, another could be to avoid the mosquitos in the first place. Knowing their flight patterns, location, and population in one area could aid in this. Additionally, classifying the mosquitos in an area would be helpful. The age and sex of the mosquito is important to find as they affect the chances of the insect carrying diseases such as malaria or yellow fever.

Many current methodologies to monitor insects are based on physical traps, but this method is not timely and cost effective. Therefore, a method of easily finding and identifying mosquitos is desired. Using LIDAR, or light detection and ranging, to characterize insects is much quicker and can identify insects as they pass through a certain area. This provides useful information in real time.

In this project, both a numerical simulation and experimental work are presented. In order to establish the effectiveness of our equipment, a MATLAB program was made to evaluate the signal to noise ratio obtained when a mosquito enters the laser beam. In addition, continuous waves of the signals initially sent and received will be compared to find a phase shift. This phase shift will then give us the distance that the insect is from the detector and therefore, the set up. Additional programs will be provided that accomplish various tasks of analyzing the signal found.

NUMERICAL SIMULATION FOR IDENTIFICATION OF INSECTS USING A CW LIDAR SYSTEM

by
Christo Videlov

A Thesis
Submitted to the Faculty of
New Jersey Institute of Technology
In Partial Fulfillment of the Requirements for the Degree of
Master of Science in Materials Science and Engineering

Department of Physics

August 2017

APPROVAL PAGE

NUMERICAL SIMULATION FOR IDENTIFICATION OF INSECTS USING A CW LIDAR SYSTEM

Christo Videlov

Dr. Benjamin Thomas, Thesis Advisor — Date
Associate Professor of Physics, NJIT

Dr. John Federici, Committee Member — Date
Distinguished Professor of Physics, NJIT

Dr. Camelia Prodan, Committee Member — Date
Associate Professor of Physics, NJ

BIOGRAPHICAL SKETCH

Author: Christo Videlov

Degree: Master of Science

Date: August 2017

Undergraduate and Graduate Education:

- Master of Science in Materials Science and Engineering,
  New Jersey Institute of Technology, Newark, NJ, 2017

- Bachelors of Science in Engineering Physics,
  Ramapo College of New Jersey, Mahwah, NJ, 2015

Major: Materials Science and Engineering

Presentations and Publications:

Christo Videlov, "Detection of an electrical signal from a single cell using carbon nanotubes", Proceedings from the NJIT Seventh International Undergraduate Summer Research Symposium, Newark, NJ, July 2014

To my family, girlfriend, and cat,
who each helped me in their own way

ACKNOWLEDGEMENT

Thank you to my thesis advisor, Dr. Benjamin Thomas, who helped me every step of the way with my thesis and in the project.

Also to Dr. John Federici and Dr. Camilia Prodan for being part of my committee.

Additionally, thank you to Adrien Genoud, Roman Basistyy, and George Willms who helped me individually with the laboratory setup, MATLAB troubles and everything else.

TABLE OF CONTENTS

TABLE OF CONTENTS
(Continued)

LIST OF TABLES

LIST OF FIGURES

CHAPTER 1

INTRODUCTION

1.1 General Statement

Mosquitos may be mere annoyances to some parts of the world, but they can be a serious threat in others. In fact, these small insects are some of the deadliest creatures on Earth. Their ability to transmit diseases through bites make them potent disease vectors. In several parts of the world, mosquitos carry dangerous diseases such as malaria, yellow fever, or the more recent Zika fever. 700 million people are affected by mosquito borne diseases every year, resulting in one million deaths annually [6, 10, 11, 25]. One mosquito species alone, the *Aedes Aegypti* is responsible for carrying several dangerous diseases.

While treating the diseases is one way to tackle this issue, dealing with the disease vector has proven to be a more effective method [19]. In order to combat this threat, insecticides and larvicides are often used to control the population of mosquitos. Monitoring mosquito populations and their flight patterns is necessary for these chemicals to be most effective.

Current population monitoring methods rely on using physical traps and bait, which can be difficult to set up in some areas and requires enough capable personnel to run the laboratory analysis. Another major limitation to this method is its statistical accuracy. The high cost of testing limits the number of assessments, which are needed to ensure accuracy. With a small sample size, there is an uncertainty in how accurate this method can be. In addition, the location that samples are obtained will have a major effect on the results, as mosquitos populations highly vary by location [19].

1.2 Alternative Methodologies and Techniques

With global climate changes, the flight patterns and species diversity of mosquitos in areas becomes more dynamic [19]. This creates issues with standard flight pattern methods, as they could become inaccurate quickly. Therefore, there is a demand for a method that will identify mosquitos quicker than current methods in the field. Identifying mosquitos out of various other types of insects that could possibly fly through the area of interest is necessary, but any information determined could be of use. Various features about the mosquito such as their age, sex, specific species and various characteristics would be of great help for disease prevention [19].

Difficulties arise from the large variety of mosquitos that exist. With over 3500 species and 41 genera of mosquitos, it would seem a difficult task to categorize them all or to see the minute differences between each. A narrower focus can be applied to species of interest when it comes to certain diseases. For example, the West Nile Virus is typically transmitted by one of the *Culex* species [6]. Specific traits of these species can be focused on in the analysis.

Finding particular characteristics such as the species or sex of a mosquito can be done by an experienced individual by eye, but this can be tedious and costly. There are more complex methods that can do this currently, but they also run into the problem in regards to cost and time. Polymerase chain reaction (PCR) is one such method that involve taking mosquitos from the wild and preparing the samples to test them. While this method is accurate to each mosquito, it might not be accurate over an area or time. Many environmental factors affect the population density and breeding grounds of mosquitos, meaning that the location where these mosquitos are obtained will affect the results [19].

Because of the long time period and cost of PCR, simply taking more samples from a larger region is not a feasible solution. A remote sensing method that can be placed in the field to obtain real time results will be much more useful to obtain such information.

Determining the age of mosquitos is epidemiologically important, as age and sex are very good indicators that a mosquito may carry disease. Only female mosquitos need to consume blood, meaning that they will be the subset of a population that is a vector of disease. Typically, mosquitos older than ten (10) days have a higher chance of carrying disease. Not many techniques exist which can determine the age of a mosquito. Ovarian dissection is one method which is used, but it is again time consuming and skilled work [19]. A method that will quickly obtain information about a more significant portion of the mosquito population would be preferred.

Therefore, a long range method that can determine many aspects and traits about insects would be beneficial. Current approaches have short comings including time, cost, and spatial accuracy.

1.3 Previous LIDAR Studies

There have been several other experiments and studies that use LIDAR, or Light Detection and Ranging, to accomplish similar goals of identifying insects or finding insect flight patterns. It is becoming more common in entomology.

One previous study done focuses on two traits, the wing beat frequency and the body to wing ratio [18]. The ratio between the body and wing size is an important factor because it is unique between several types of insects and can be used to characterize signals.

Using only those two characteristics has a few limits, namely that some mosquitos and insects have overlapping traits, making these two qualities insufficient in absolute characterization of specific mosquitos. Thus, they cannot be the only definitive methods of identifying specific types of insects, and more parameters must eventually be introduced.

Several of these papers do not focus on small mosquitos, as done in this thesis. One in particular observed many different types of large insects using long distances up to 140 meters [18]. Mosquitos listed here had a wing cross section almost ten times larger, with a slightly larger body cross section compared to what is used in experiments in this thesis. Classification was done using mainly wing beat frequency and body to wing ratio.
These previous studies had a focus on the time of insect's flight, whereas this thesis will try to attain information from the signals to be used for future classification.

1.4 Objective

The objective of this thesis is to study the use of LIDAR in remotely identifying and characterizing mosquitos, using both numerical simulation data and a laboratory experiment. In this thesis, numerical simulation and MATLAB (Matrix Laboratory) simulation will be used interchangeably. The purpose of the numerical simulation is to mimic realistic results using a model based on theoretical formulas and values. As equipment can be expensive, having an idea of the feasibility of this project is important. A numerical model will give vital information regarding the effectiveness of LIDAR in characterizing insects. For example, as the distance between the mosquito and the photodetector used to capture the signal increases, the strength of the signal decreases. Knowing the distance at which the system is effective is useful, especially for future

outdoor experiments. From previous scientific contributions and literature [24], variables useful to the model are known. Knowing specific elements of the experiment such as the collecting optics and distance to the insect gives enough parameters to create an accurate representation of the signal that would be received.

Initial experiments are done in a laboratory setting as a proof of concept, and to find how the experiment could be improved. Finding sources of errors, the signal to noise ratio, and limitations of the system to accurately retrieve optical properties of mosquitos are vital steps in finding how effective LIDAR could be to remotely characterize mosquitos. In addition, the optical properties and wing beat frequency of mosquito species and various types of insects will help in the future when classification becomes more important, and a database must be set up for the remote identification of insects using LIDAR.

CHAPTER 2

LIDAR AND REMOTE SENSING

2.1 LIDAR Methodology

Consisting of a laser and a photodetector, LIDAR is used in many fields such as atmospheric physics, geography, laser guidance, and many more. These devices are effective at detecting the distance from a target to the detector. Usually this is done using a pulsed laser, where the difference in time of flight of the pulse is measured between the initial pulse and the received pulse. The light must travel to the target, reflect, and then travel back to the detector, so the distance is multiplied by two in Equation (2.1). In this equation, *t* is time and *c* is the speed of light.

$$t = \frac{2d}{c} \tag{2.1}$$

One typical use for LIDAR is mapping topography, where a laser is mounted under a plane and swept over an area in order to measure the distance from the terrain. Knowing the height of the aircraft and principle axes, it is possible to map the terrain measured. It is also finding use in autonomous vehicles to detect the area around them and distance between other vehicles. As mentioned in Section 1.3, LIDAR has been used in similar studies for the purpose of insect flight patterns.

The surface of the target is of great importance to any laser use. The target and its surface determines how much of the laser light will be reflected back. Factors such as the size of the target and how reflective the target is are two of the most important values.

Cross section will be used rather than size of the target, as the cross section is indicative how much of the surface interacts with the laser light.

The surface of a mosquito is not a diffuse Lambertian reflector, that is to say, it does not scatter reflected radiation in all directions equally. The amount of light reflected is defined by the reflection and backscatter coefficient which includes both specular and scattering reflection. The solid angle of the collecting optics and reflectivity will largely determine the amount of light reflected back.

In order to collect as much reflected laser light as possible, a 3-inch diameter parabolic gold mirror is used to collect and focus the light into the detector's active area. As gold is highly reflective in the near and short range infrared region, it is an ideal material.

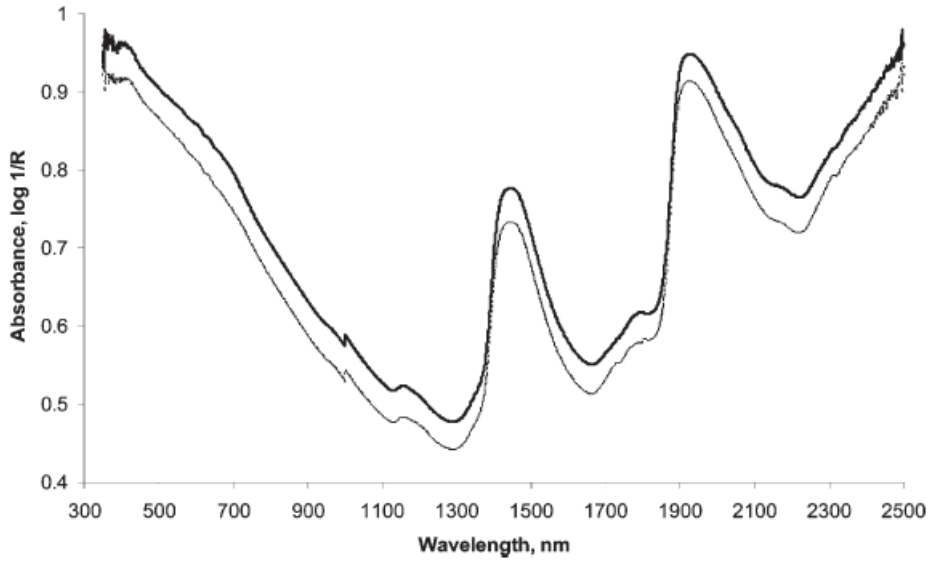

Figure 2.1 Absorbance spectra example. The absorbance of *Anopheles arabiensis* (top) and *Anopheles gambiae* (bottom) mosquitos is shown here. Although we are used an *Aedes Albopictus* and *Culex* species, the result will be similar.

Source: [19]

The wavelength used is 1.32 μm because mosquitos and several other insects have a high reflectance in that region. Figure 2.1 shows one spectra graph of a mosquito, with high reflectance around 1.3 μm. This allows the strongest possible signal reflected back. In this section, many limitations have been mentioned which lower the signal to much weaker power compared to the initial laser power. One of the purposes of the numerical simulation is to determine whether enough light can be detected to form a useful signal.

2.2 Formula and Terms

In this report, a constant power laser is utilized. Therefore, no modulation occurs and no range finding is done. Section 2.5 will describe the power once it is modulated for range finding use. The actual power is calculated and described in Section 4.1.

The reflectivity is wavelength dependent. Although Figure 2.1 describes the absorbance spectra for one species of mosquito, other sources indicate that the value is between 20% and 60% [13, 18].

As mentioned, some light will reflect diffusely off the insect. This means that out of all the reflected light, only a fraction can be collected. Equation (2.2) is used to describe the power that is received. $I(d)$ is the light intensity received back from the mosquito.

$$I(d) = \frac{K}{d^2} * I_0\left(t - \frac{2d}{c}\right) * \frac{c_b * \beta_b + c_w * \beta_w}{\pi * (r + div * d)^2} \tag{2.2}$$

c_b and c_w are the cross section of the mosquito's body and wing respectively, while β_b and β_w are the backscatter coefficient for the mosquito's body and wing. $r + div * d$ accounts for the change in the radius of the laser's beam over distance where r is the initial

radius of the laser beam, div is the divergence of the laser beam over distance, and d is the distance between the Photodetector and the mosquito target. K describes the solid angle of the parabolic mirror. This also includes the reflectivity of any optics in the experiment, including the three gold mirrors. Equation (2.1) is included here to account for the time the light spent traveling before it reaches the detector. Equation (2.2) does not completely describe the experimental set up and signal we receive. Most of these restrictions stem from the laser, and how the spatial beam profile of the laser changes the power that reaches the mosquito. This is defined in more detail in Section 3.2.

2.3 Classification

When an insect passes through the laser beam and a signal is received, several pieces of information are obtained. Putting these pieces of information together will hopefully allow classification of signals recorded by mosquito or insect with a degree of certainty. While trained individuals may be able to identify insects through sight, a program must be written to categorize insect signals received. Insects have several identifying traits that will be used.

The easiest trait is the wing beat frequency. As the mosquito flies through the beam, it will flap its wings. When the wings are completely up or down, they will appear very different compared to when they are parallel to the body of the mosquito. This will appear in the signal as wavelike oscillating behavior. In many insects, the wings are of comparable size if not bigger than the body. These wing beat signals should be clearly visible over the body contribution in the signal. Many other insects have frequencies in the same range as mosquitos [18]. Mosquitos in particular have a unique wing beat which they use in their

flight which is described as leading edge vortices and trailing edge vortices [2]. If this rotational mechanism is visible in signals, it could help in identifying mosquitos. Figures 4.7 and 4.8 display the projected area during flight from two perspectives.

If the wing beat frequency can be retrieved, then the body to wing ratio can also be calculated. Depending on the direction that the mosquito is facing relative to the laser beam, its body to wing ratio will appear differently in the signal. Figure 3.2 shows mosquitos in various orientations. Although this body to wing ratio varies, it could still be a useful tool. Not only will the body to wing ratio be found for the purpose of identifying the insect or mosquito, but additionally the orientation of the mosquito might be possible to extrapolate.

These are two of the main tools used to identify and characterize the signals of insects. Through the experiment, more details are found analyzing the signals that might be useful to characterize the insects. For example, the wing beats appear differently through many signals, possibly allowing more information to be gained about the flight of the insect.

2.4 Range Finding

A useful tool in classifying insects is to understand the distance where they pass through the laser beam. Although not yet used, it is important to understand how it will impact the results later on. Knowing the distance, along with the strength of the signal can give a good idea of the size of the source. Without this, trouble can arise from situations where larger insects that are further away from the laser compared to smaller insects result in signal with similar strength. The method of determining the distance will use the phase shift of a

continuous wave signal to determine the time of flight of the laser beam, as opposed to the pulsed light that is common in LIDAR use. It is described in Equation (2.3).

$$I_0(t) = \bar{I_0} \cdot (1 + \mathrm{A} \cdot \cos(2\pi f_L t)) \tag{2.3}$$

$\bar{I_0}$ is the mean power that the modulation oscillates around, while A influences the height of the amplitude. f_L describes the frequency that will be used in modulation. This value must be lower than the bandwidth of the detector, while large enough to obtain meaningful distance measurements.

One main change compared to past studies done comes from the method of which range finding is done. While the IR laser beam uses the phase shift to measure the distance between the insect and the detector, an alternative method commonly used is based on the Scheimpflug principle. For more detail on the range finding using the Scheimpflug principle, see the following papers [3, 4, 5, 18]. No modulation is required using this method, but the distance given by this method is usually a range.

An example of how phase shift is used is shown in Figure 2.2. The initial signal follows Equation (2.3), while the received signal is one where no power is lost for the purposes of showing the phase shift. From Equation (2.1), the distance can be found.

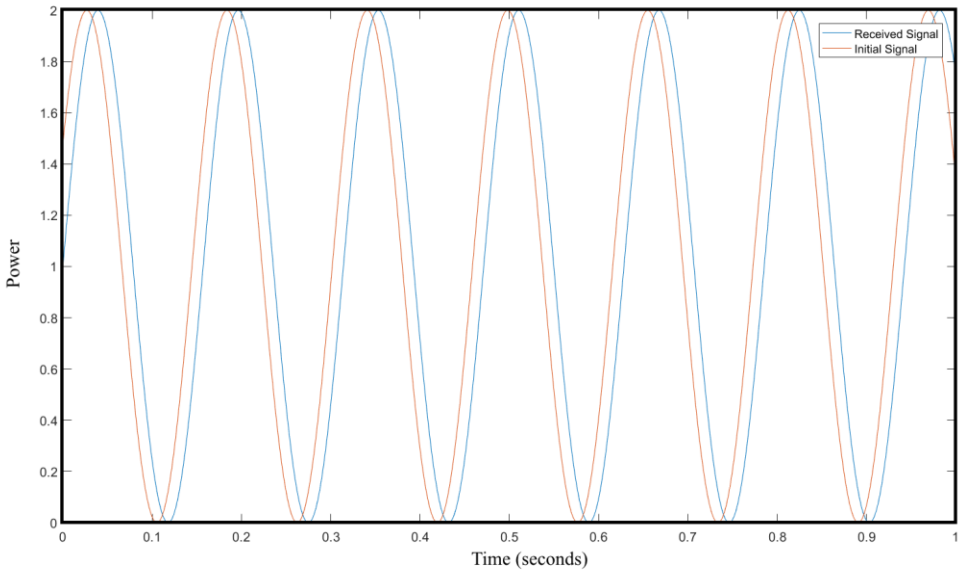

Figure 2.2 Representation of the phase shift. Sources of error in determining the distance comes when noise is introduced and from hardware limitations in bandwidth. As more noise is present, the position where to compare waves becomes less clear. The time of flight is used to determine the distance.

The signal can be characterized as a sinusoidal wave with modulating power. Although the speed of light is extremely quick, it still takes time to travel and return. An example of a modulated signal is shown in Figure 2.2, where an initial signal is sent, then after some time, a signal is received. The signal received will have noise from the background and detector, and a visible body and wing contribution from the mosquito. In this theoretical signal, the modulation of frequency from the initial signal will be seen. In experiments where we measure the *Aedes Albopictus*, the acquisition system uses a bandwidth of 30,517 Hz. Using Equation (2.1), we see that the absolute spatial resolution would be approximately 4912 meters.

This is too large to be of any use. However, these measurements are only being used to detect the wing beat frequency and body to wing size, so a higher degree of

precision is not needed. In future testing, the gain step will be lowered to 0 or 10 so that range finding can be done. The bandwidth present on the 0 and 10 gain step is 10 MHz and 4 MHz, respectively, which have an absolute spatial resolution of 14.99 and 37.47 meters, respectively. While still very large, using averaging and a Hilbert transformation will allow further precision. Improving the accuracy of range finding is also possible using methods such as the heterodyne technique [3]. If a precision within a meter is possible, it would be helpful in aiding with the characterization of insects.

Typically a transformation is used to measure the phase shift. The angle between the initial signal and the received signal describes the phase shift present. Results of the numerical simulation phase tests are summarized in Section 3.4.

CHAPTER 3

NUMERICAL SIMULATION

3.1 Purpose

There were several outcomes obtained from the numerical simulation. However, three of them were of high importance. The signal to noise ratio vs distance, the phase shift vs. distance, and the amplitude of the initial signal. The signal to noise ratio would give information about how much signal we would ideally be receiving over the noise. Considering the small portion of light that would return compared to the initial laser light sent by the laser, this value is very important. It is necessary that we are able to see the mosquito's signal sufficiently over the noise present from the laser, detector, and background. A ratio above ten is typically desired. Prior to choosing the Thorlabs PDA20CS Photodetector, this numerical simulation was also used to test the effectiveness of each possible detector option. Once the PDA20CS was selected and tested, each gain step was tested for the three previously stated values.

This information could give an idea of how well the detector would work both indoors in the laboratory setting and outdoors for possible field measurements. While the PDA20CS is being currently used, another Photodetector, the PDA10T, was found that would possibly be better suited for the longer distances in an outdoor setting. However, a much higher cost makes it unwarranted for indoor use.

Each gain step increases the gain by a large factor, while slightly increasing the noise. Therefore, the signal to noise ratio increases with each gain step. The tradeoff with each increase in gain step is a loss in bandwidth. This loss would make phase measurements

less accurate. Therefore, a compromise must be made here between precise distance measurements and signal strength. As previously mentioned in Section 2.4, the amount that we modulated the power of the initial laser is also a variable which must be found. The accuracy of the phase shift measurements is related to the amplitude of the laser power. As amplitude decreases, the influence noise has on the modulation becomes more apparent. When the amplitude is larger, it is easier to correctly identify the sine wave from modulation, which the Hilbert transformation used for phase shift relies upon.

3.2 Assumptions

Several assumptions are made in this simulation. This is necessary for a numerical experiment to be done as there are many variables which cannot be accounted for precisely. Some aspects of the experiment are random and changing every iteration, while others cannot be found without specialized equipment. One example is the power of the laser beam throughout its cross section, which is commonly referred to as the laser beam spatial profile, or Gaussian beam. Many lasers have a similar profile such as in Figure 3.1.

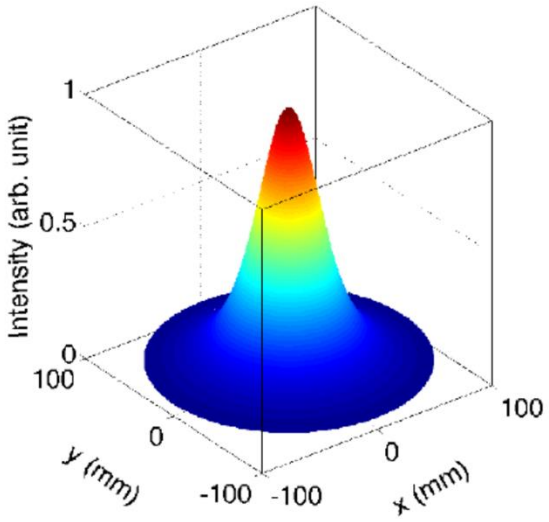

Figure 3.1 Typical Spatial Beam Profile. This three dimensional graph shows an example of the Gaussian spatial beam profile of a laser. In the very center of the beam, its intensity is at its highest, while it decreases further away.

Commonly, the intensity of the laser beam is greatest in the center of the laser beam cross section, with the intensity decreasing further from the center. As the mosquito will be flying in a straight line through the middle of the laser beam, a two dimensional equation is sufficient. Flying at a constant speed, the equation is able to be converted from power vs. distance, to power vs. time. This allows a Gaussian profile to be used in the simulation. This will be visible in signals as mosquitos traveling in the beam will reflect varying power depending on their location in the laser beam profile.

As stated, the insect is assumed to fly straight across the center of the beam once each iteration. There are no turns or changes to the direction of its flight. The top speed of a mosquito is estimated at 120 cm/s (1.2 m/s) for some species, but as that is extremely quick, we will assume the speed of mosquitos to be 2 km/h, or 0.555 m/s [23]. This will be used to determine the time the mosquito will spend in the beam, or transit time, if it flies straight across. At 4 meters, with a laser beam diameter of 16.7 mm, the mosquito would

have a transit time of 0.03 seconds which gives about 18 wing beats assuming every wing beat is positioned in the cross section of the laser beam. Laboratory experiments will likely give different values, as the mosquitos will be travelling at various speeds. Experimental signals showed mosquitos in the laser beam for longer periods of time than assumed here.

Because of the large possible range seen in the reflectivity values of the mosquito from 20 to 60%, a specific value is difficult to assume. Therefore, the middle value of 40% will be used in the simulation.

The orientation of the mosquito relative to the laser beam must be taken into consideration as it affects the cross section of the body and wings. Two different orientations are considered in this simulation. One is sideways, where the mosquito flies directly across the laser beam, similar to the mosquito on the right in Figure 3.2. The second is flying vertically with respect to the laser beam. The wing contribution changes the most between orientations. When the mosquito is sideways, only one wing is seen as it flaps, whereas when the mosquito flies vertically, both wings can be seen, multiplying the wing cross section by two. While this is a simplification of the mosquito's flight mechanics, it is considered sufficient for the purposes of the simulation.

Figure 3.2 Several mosquito orientations. The appearance of the wings in the signal is highly dependent on the orientation of the mosquito when it is in the laser beam. In this photo are three possible orientations of the mosquito, each showing a different cross section to the laser beam.

Source: https://www.youtube.com/watch?v=JQl4OP2XdYA [2]

The average wing beat frequency of male and female mosquitos is different depending on the species. Using *Aedes Aegypti* as a reference, male mosquitos have a frequency of 711 Hz, with a standard deviation of 78 Hz, and females having a frequency of 511 and a standard deviation of 46 Hz [1]. In this numerical analysis, we will assume a frequency of 600 Hz for the hypothetical insect, in between the two sexes. Many different species have a wing beat frequency that is quite similar.

The noise from the detector is assumed to be Gaussian distributed. Several measurements of only the detector noise were obtained using the Tektronix MDO2042C oscilloscope. The active area of the detector was covered with a provided cover so no additional noise was received from any background light sources. The Snapshot function was used which gave several values including the maximum, minimum, mean, and Root Mean Square (RMS) values of the detector noise. Four trials were done, and the average

of each respective value was taken. Using the randn function, a random number generator, in MATLAB, a random Gaussian distribution was made with values that most matched the values obtained of the noise. Experimentally, more noise was received than expected because of two parts of the experimental set up. In order to match this new increased value, the noise was multiplied by 6. No baseline is used, as the baseline changes several times, from optimizing and improving the experimental set up.

3.3 Inputs and Equations

Several values for the initial laser power, I_0 are tested. To more closely match the experimental set up, a constant power of I = 3.75 Watts is chosen. However, when running tests on the effectiveness of phase shift measurements, Equation (2.3) is used as the initial signal. Several values of $\overline{I_0}$ and 'A' are chosen making the power modulate from the lowest of 3-4 Watts, up to 3.8-4 Watts. The power received is similar to Equation (2.2).

The one difference is a factor P which accounts for the Gaussian spatial beam profile, and how the mosquito occupies an area of the total laser beam cross section. This multiplies all of Equation (2.2) by a Gaussian function.

If the mosquito travels through the widest part of the beam, as assumed, then the Gaussian beam spatial profile can be viewed as a two dimensional profile, rather than three dimensional, as in Figure 3.1. It will resemble a typical Gaussian distribution as a function of power and distance in the x direction. Because the mosquito is travelling at a constant speed, and assumed to enter the beam at the same time throughout the simulation, this two dimensional spatial beam profile can converted from a unit of distance, to one of time.

Using a ruler to measure the body of a laboratory mosquito, and assuming an eclipse shape for both the body and wing, the body cross section was estimated as 2.6 mm^2, and the wing cross section as 0.8 mm^2 each wing. The radius of the laser beam is measured as 12.7 mm, or half an inch. Divergence has the value previously mentioned, 1 mrad, at a distance of 3.6 meters from the detector.

All previously stated signals, I, have the units of Watts. Using the responsivity and gain specifications of the photodetector, the signal can be converted in Volts. Appendix A includes all gain step specifications. According to the manufacturer, responsivity is about 0.85 A/W at 1300 nm.

In order to be more accurate, the results of the experiment were compared to that of the simulation to see possible sources of error in order to further calibrate the simulation. One important correction came from the shadow of the sending mirror in front of the sending mirror. To allow the laser beam and collecting optics to be co-axial, a sending mirror must be placed in front of the parabolic mirror. This results in some of the reflected radiation being blocked by the sending mirror and its post from reaching the parabolic mirror and ultimately reaching the detector. After accounting for a lower collection of light, the results closer matched that of experiments.

3.4 Simulation Results

A basic output of the numerical simulation is included in Figure 3.3. As stated, in the middle of the mosquito's signal, the signal is at its highest, where the laser beam spatial profile is at its strongest.

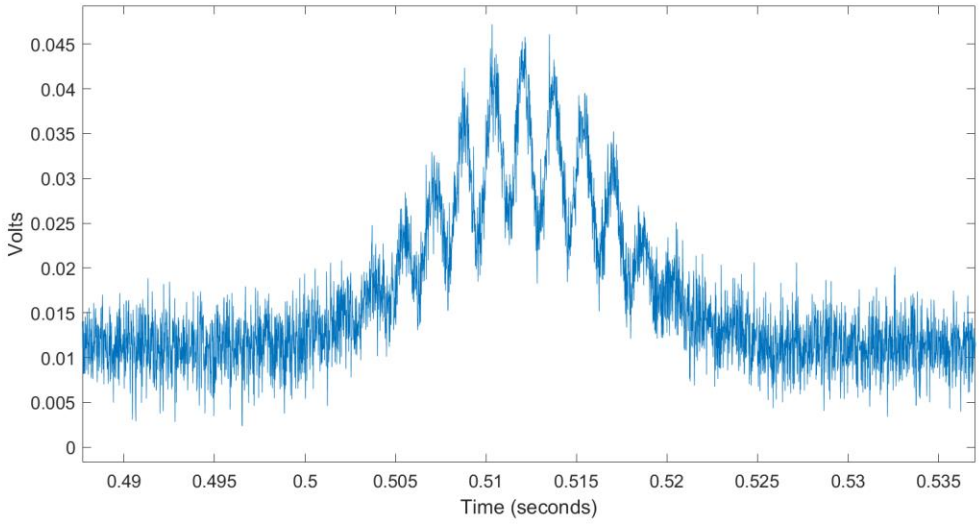

Figure 3.3 Simulated LIDAR Signal at 3.6 meters, the middle distance in the experimental set up. The baseline is set at zero, compared to the experiment, where the background will introduce a baseline noise. The gain step simulated is 50 db. The SNR found here is 11.8.

Two different transit times were used in simulated results. One assumes the mosquito travels at 0.555 mph, and one that has the previous transit time multiplied by four, as used in Figure 3.3. An increased transit time was introduced after experiments were done, because transit times ended up being longer than anticipated.

The signal to noise ratio is the first value of importance obtained from the numerical simulation. It is calculated as the ratio of the maximum value of the signal over the standard deviation of the noise. Two conditions are used, one using the indoor laboratory conditions of the experiment, and another outdoor setting.

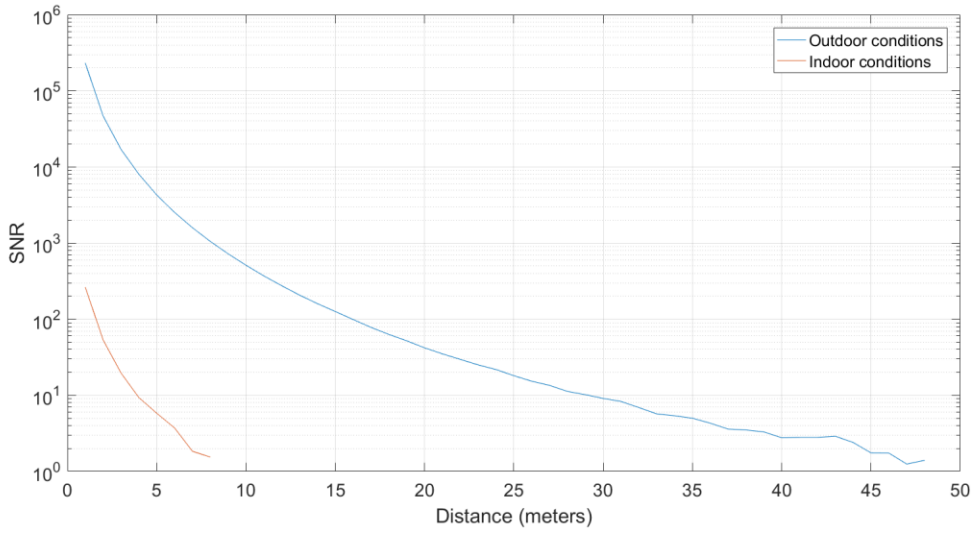

Figure 3.4 Simulated Indoor and Outdoor SNR. The main results here are the maximum distance where useful results can be obtained.

In an indoor setting, SNR will reach 1 after 8 meters. As the outdoor setting will have different conditions, several parts of the experiment will be changed. The simulation will assume a larger parabolic mirror in use that is 10 inches in diameter, which is used for the further distances needed experimentally outdoors. In addition, as a large part of the noise comes from parts of the set up and background in the laboratory, the outdoor set up will assume no further noise apart from the photodetector. These aspects that increase the noise are specified in Section 4.1.

The outdoor results show a much further distance possible than using indoor conditions. After 45 meters, SNR is around 1. This is a distance more than 5 times further. These results show an adequate range if this system was to be used outdoors.

Early results in the numerical simulation show that the Hilbert transformation is more effective than the Fourier transform in this application. It is similar to a Fourier transformation, which is commonly used to measure the phase in signal analysis. One

setback with the Hilbert transformation is that it requires a high signal to noise ratio. A gain setting of 10 is used in the numerical analysis of the phase shift, with 200 kHz modulation for Figures 3.5 and 3.6. A larger mosquito cross section is used from "Observation of Movement Dynamics of Flying Insects Using High Resolution LIDAR" [18].

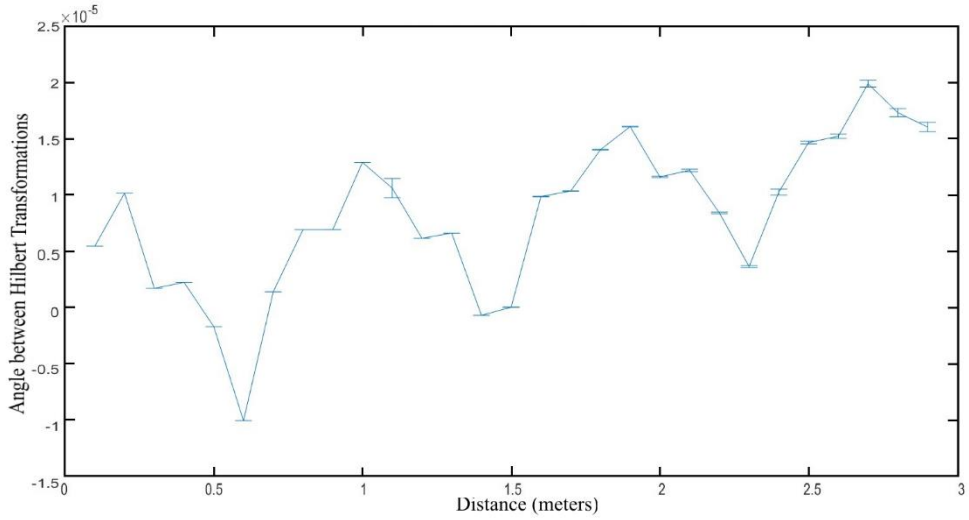

Figure 3.5 3.8-4 Watt Amplitude Phase Shift. Using a smaller amplitude resulted in multiple distances having the same phase shift result. While there was an upward trend with distance, this would be unusable and gave information that a larger amplitude was necessary.

Using an amplitude from 3.8 to 4 Watts, the smallest tested amplitude, results showed that a larger amplitude would be necessary to determine the distance. Although there is an upward trend in phase shift with distance, this amplitude would not allow distance to be accurately measured.

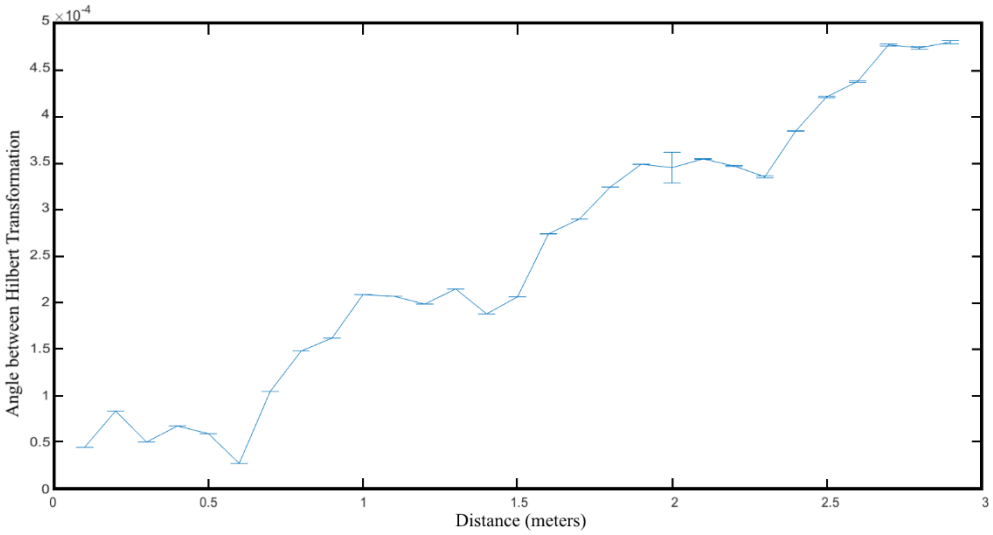

Figure 3.6 3-4 Watt Amplitude Phase Shift. A larger amplitude showed much more promising results, with clearer upward trend with distance. However, there was still results that had the same phase shift with different distances.

With a greater amplitude of 3 to 4 Watts, phase shift appeared to vary more with distance, but still not sufficiently. A slightly greater amplitude will be necessary in laboratory experiments. The same value of the angle between transformations is given for several distances, which makes it unsuitable. As modulation was not in use, no further tests were ran to establish a proper amplitude range. Further tests would have used a modulation of 2.5 to 4 Watts.

3.5 Discussion

While Figure 3.3 allows a wing beat frequency to be determined, experimentally it is likely to be much higher. This is because the mosquito may start out stationary within several inches of the laser beam, not allowing the insect to build up speed, causing it to fly through the laser beam for longer periods of time. In addition, it will likely not only travel directly

across the beam, but in many different directions, some of which result in a longer transit time in the beam.

As many numerical simulations make assumptions and take values from other sources, there are many sources of error. There are multiple differences between the simulation and experiments, which account for the differences present. All cross section measurements are done with a ruler, including the mosquito and laser beam radius. The mosquito's small size makes accurate measurements more difficult, while the laser beam is not in the visible wavelength, making infrared sensitive cards necessary to see its size. Only one male *Aedes Albopictus* mosquito was measured with a ruler to determine its size, while females and males, and each individual species have different sizes.

A wide range in backscattering coefficient introduces another source of error, as the backscatter combined with the cross section of the insect give a high possible error in Equation (2.2).

In future experiments that might be done outdoors, it can be assumed that there will be less noise. Calculating how much noise is difficult. Two parts of the laboratory set up that will be expanded upon later, the slanted glass and beam stop, introduce more noise to the signal. However, these are necessary to the indoor experiment, and will most likely not be included outdoors, or be placed much further away. With less noise present in the signal, a higher SNR will be possible for further distances.

CHAPTER 4

EXPERIMENTS

4.1 Optical Layout and Specifications

The optical set up uses three separate mirrors, two of which are outlined in Figure 4.1. One sending mirror, not shown in Figure 4.1, is between the converging lens and sending mirror shown in the figure. An off-axis parabolic mirror collects the radiation which is scattered from the mosquito, while the two sending mirrors are used to position the laser beam properly. This parabolic mirror is the K variable that was previous discussed in Section 3.3. The mosquitos are placed in a long plastic tube, approximately 1.2 meters in length, which has three circular holes drilled in it. These are used for blowing air into, as mosquitos are generally stationary without stimuli. The distance from the parabolic mirror to the beginning of the tube is 2.98 meters. At the end of the tube, a beam stop is placed, which is highly absorptive of infrared radiation.

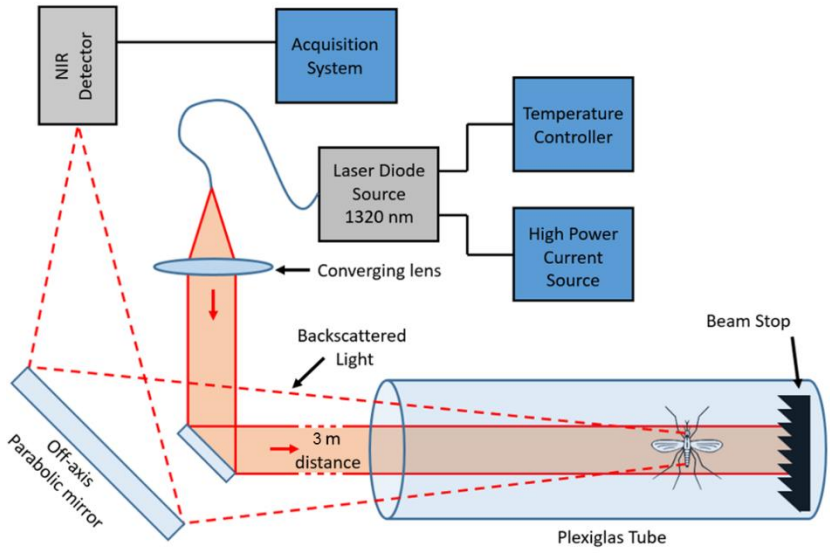

Figure 4.1 Optical Layout of the system. A borosilicate glass is placed at the front of the Plexiglas tube to prevent escape.

Two species of mosquito tested so far were *Aedes Albopictus* and an undetermined *Culex* species. Their sex can be easily determined visually based on body size and bushiness of their antennae. The males have much more small hairs (fibrillae) on their antennae and smaller bodies than the females. Mosquitos are inserted approximately 3.6 meters from the detector following the path of the beam. A large distance allowed multiple measurements with a variety in strength of signal.

To double check on the power of the laser, an optical power detector was used. The power of the laser is not constant, as it has some degree of noise, and changes with temperature caused by the temperature controller and stabilization. As we used about 3.6 Watts of power, we could not measure the power directly using this detector. It had a limit of 1 Watt maximum power detected, so a different approach was used to measure the power of the laser. An attenuator glass filter with low transmission at the infrared range was used. Two Amps of current were applied to the laser, which put the power well within the 1 Watt maximum power limit. This resulted between 0.7196 and 0.7395 Watts of power measured, changing over time. Placing the low transmission glass between the laser and detector resulted in a power of 85.18 mW measured, which is between 11.565% and 11.837% of the total power. Using the 10 Amps that were used throughout the experiments, a signal with the attenuator glass filter results in between 0.4279 Watts and 0.434 Watts of power measured. This means that in the experiment, the power wavered between 3.6148 and 3.75 Watts. This wavering of the laser power was not sudden, but appeared slowly as the temperature was stabilized.

As the worry of mosquitos escaping grew larger, more measures had to be taken to prevent it. The beam stop was placed on the back of the enclosure to prevent escape from

the back of the tube, and a borosilicate glass was placed in the front of the enclosure. However, a reflectivity of 10% in the infrared range caused saturation in the detector. To remedy this, the glass was slanted down, causing any reflection of the glass to not be recorded by the detector. A 3-D printed cover was placed between the glass and the tube to fill the gap.

Moving the parabolic mirror over, to prevent the shadow of the sending mirror and post was tested briefly, but results were not much better, so the original set up remained.

While a sufficiently high bandwidth is necessary for phase measurements on the other of Megahertz, it is not needed for early experiments. For the preliminary experiments, other factors are observed such as the wing beat frequency, body to wing contribution and other characteristics in the wing beats. According to the manufacturer, the 50 gain step has a gain of 238 kV/A with a bandwidth of 67 kHz. The acquisition card uses a bandwidth of 30,517 Hz, which is more than enough to measure the wing beats of the mosquitos, which should be no more than 850 Hz. Additionally, the software that uses the acquisition card used to record results was unable to record measurements with extremely high bandwidth at the time of this report.

4.2 Results

Three total batches of mosquitos were received from the Center of Biology Vector at Rutgers University, the first and third batch of only *Aedes Albopictus*, and the second batch containing *Aedes Albopictus* and a *Culex* Species.

Figure 4.3 is an example of a mosquito sighting that was recorded. Sharp peaks were typically seen indicating mosquito wing beats.

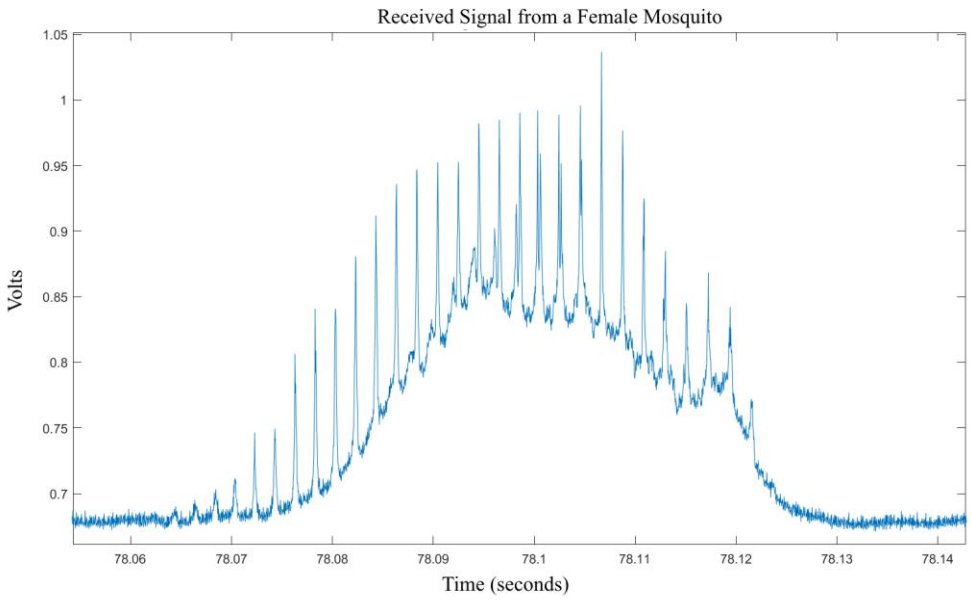

Figure 4.2 Signal received from a female *Aedes Albopictus* mosquito. The wings appear to be enter the beam before the body, and its orientation allowed for very prominent, sharp wing beats to be seen.

In several mosquito sightings, sharp peaks were prominent where the wing beats were. The mosquito body appeared as expected, rising and falling gradually in the signal. The frequency of the wing beats was found using the Fourier transformation of the signal.

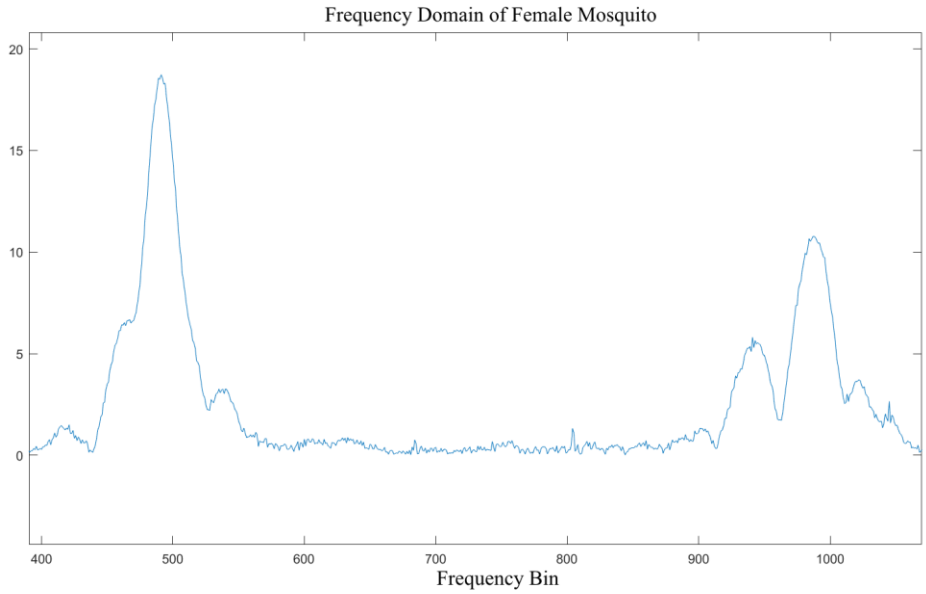

Figure 4.3 Absolute value of the Fourier transformation of Figure 4.2. Looking at the maximum value between the ranges where mosquito wing beat frequencies are known to be, the frequency can be identified as 491 Hz. Multiple harmonics can be found in higher frequencies, seen at around 1000 Hz.

This Fourier transformation allowed the wing beat frequencies of all signals to be recorded. A signal from a male of the same species is included which shows the difference in wing beat frequency and the difference possible in signals.

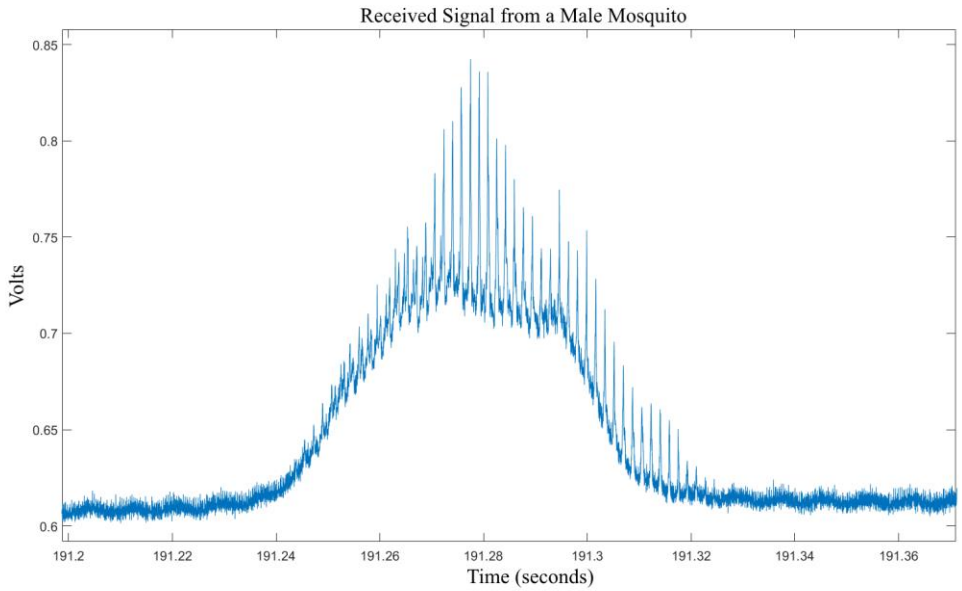

Figure 4.4 Signal received when a male *Aedes Albopictus* mosquito flies through a beam. The body to wing ratio is not constant through the signal, lower in the beginning of the signal, but growing near the middle. A frequency of 560 Hz is measured.

There are multiple patterns that are visible in the wing beats, such as peak sharpness, body to wing ratio, and change in frequency over a single signal. These can be indications of orientation, speed, or some other aspect of the mosquitos. As seen in Figure 4.5, multiple patterns exist for mosquito wing beats. They have been narrowed down to four main categories. One is the sharp narrow peaks already seen in Figures 4.2 and 4.4. Another is a dull wide peak seen in graph B of Figure 4.5. There are also peaks that clearly have a smaller secondary peak that appear after the main sharp or double peaks mentioned. These will be split into two more categories called sharp/double and dull/double.

Sharp peaks that occur come from specular reflection off of the wing of the mosquito [4, 5]. When the wings are normal to the path of the laser, specular reflection is being captured as opposed to the usual diffuse reflection. Specular reflection is much stronger than diffuse reflection, causing the increase in signal strength in short time periods.

This type of wing beat is visible among all of the mosquitos measured and is present in the majority of signals.

In the first batch of *Aedes Albopictus* measurements, there is a wavelike behavior in the noise that appears. We have attributed this noise, which has a frequency of 120 Hz to the lights that were on in the room. In further measurements, the lights were turned off at the time of recording.

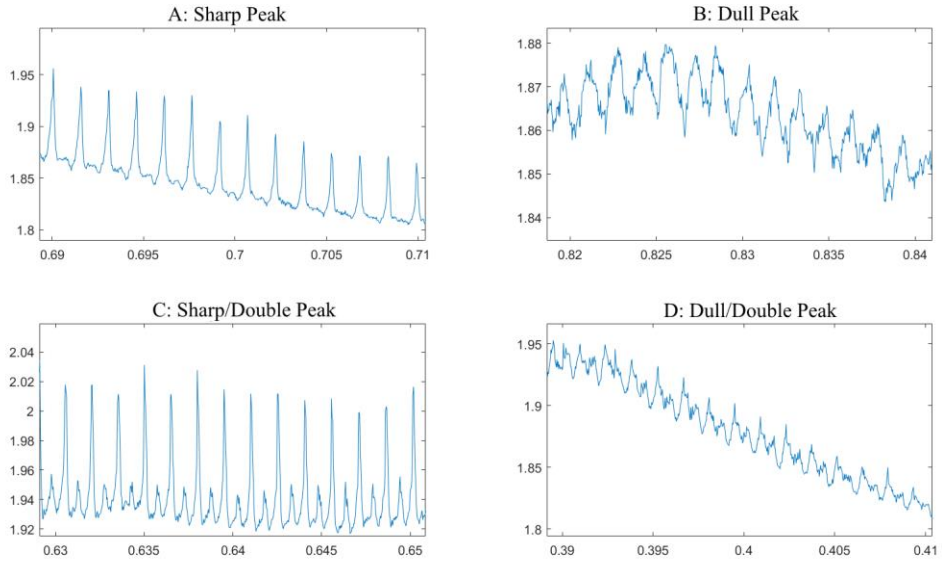

Figure 4.5 Four Different Peak Types, Voltage Vs. Time. A) represents a sharp peak type, occurring when specular reflection is detected. B) represents a dull peak, occurring less often than sharp peaks, and is caused by diffuse reflection. C) and D) depict a second peak that is visible after each main peak. All signals are from a male *Aedes Albopictus* using the same time scale.

Specular reflection occurs when the light travels back at the same angle that it is sent. Because of the sending mirror that is in the way of the parabolic mirror, this angle is not exactly 180 degrees. As the wing must be in a certain position to cause the specular reflection, we assume that these sharp peaks indicate that the mosquito is in a certain position with respect to the laser beam.

In order to obtain more information about where this specular reflection could come from, all of the mosquito signals were categorized to five types of peaks. All of this categorization was done by eye. The 'other' category was reserved for signals that were different enough from the other categories that they did not fit them but did not have any significant pattern to place them in their own category. Signals where no wing beat frequency was visible or hard to differentiate from the noise were ignored.

Table 4.1 Characterizing Wing Beat Peaks

	First Batch		Second Batch & Third Batch			
	Aedes Albopictus		*Aedes Albopictus*		*Culex* Species	
	Male	Female	Male	Female	Male	Female
Sharp Peaks	3 (25%)	6 (66.6%)	15 (14.56%)	5 (12.5%)	15 (57.7%)	12 (30.77%)
Dull Peaks	2 (16%)	1 (11.1%)	19 (18.44%)	5 (12.5%)	2 (7.7%)	9 (23.08%)
Sharp double peaks	1 (8.33%)	1 (11.1%)	54 (52.43%)	24 (60%)	4 (15.4%)	13 (33.33%)
Dull double peaks	1 (8.33%)	1 (11.1%)	15 (14.56%)	4 (10%)	2 (7.7%)	4 (10.26%)
Other	5	0	0	2	3	1
Total	12	9	103	40	26	39

The majority, 67.4%, of all visible wing beats are, or have a majority of, sharp or sharp double peaks. As a change in orientation occurs sometimes when the mosquito is in flight, the type of wing beat peaks will change in a single signal. For example, Figure 4.5 A and B are from the same mosquito sighting. The first batch is separated from the second and third batch because mosquitos from the first batch were introduced from the side using a small tube to place them directly into the laser beam. Mosquitos in the second and third batch were placed in the tube, where they could fly freely in multiple directions during recording. As this likely influences their orientation when a signal is recorded, they are

separated. Discounting the first batch, 68.6% of freely flying mosquitos register a sharp peaking wing beat.

As previously stated, it is believed that the different types of peaks correspond to a different orientation of the mosquito in the laser beam. When the body to wing ratio is observed overall, it appears to have a very wide range. However, as the body to wing ratio is connected to the orientation as well, it makes sense that there is more order when the ratios are split into categories.

Table 4.2 Male Aedes Albopictus Body to Wing Ratio

Type of Peak	Sharp	Dull	Sharp/Double	Dull/Double
Average	1.2081	4.8535	1.4294	5.2368
Standard Deviation	0.9401	2.3174	0.912	3.028

Table 4.3 Male Culex Species Body to Wing Ratio

Type of Peak	Sharp	Dull	Sharp/Double	Dull/Double
Average	1.4785	2.2769	0.7294	3.9279
Standard Deviation	0.70218	0.0895	0.422	1.901

A computer model was made which replicated the unique flight pattern of a mosquito. Using this model, the projected area of the insect was calculated and plotted. This shows how the body to wing ratio and wing beat peaks can change as the orientation is different.

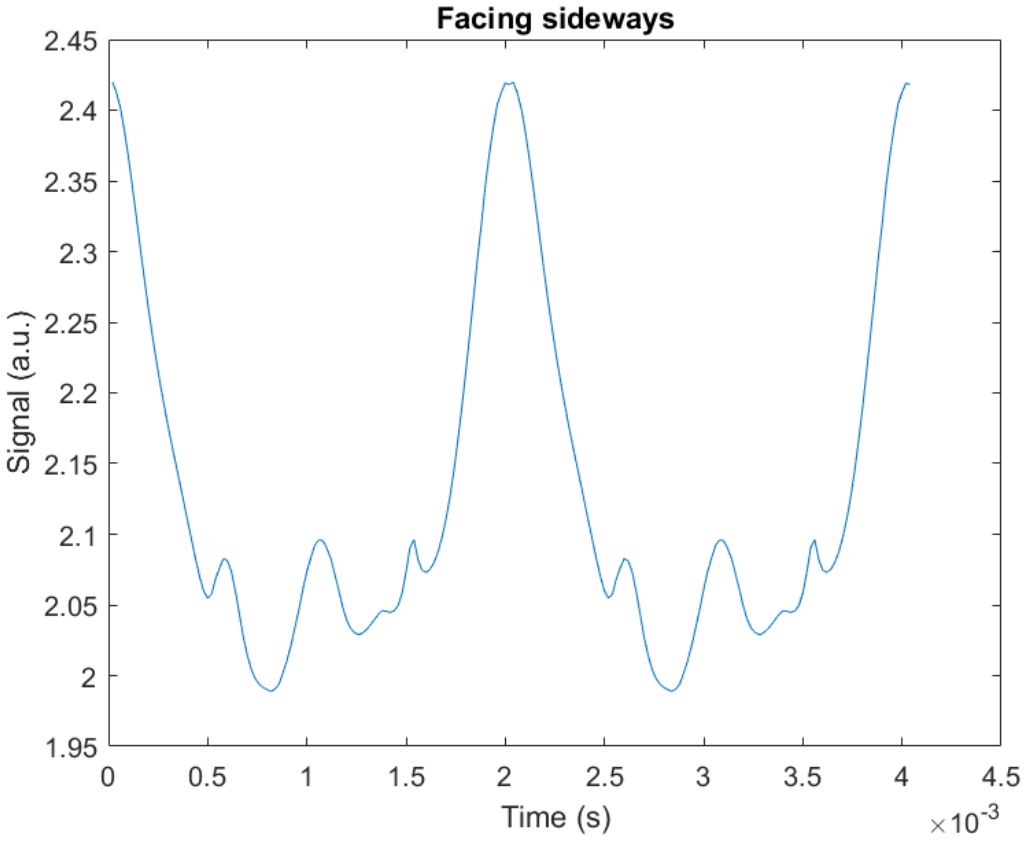

Figure 4.6 Projected area of a mosquito using a side view of a mosquito over two full cycles. This assumes that the mosquito is facing sideways such that it crosses the laser beam. Very small peaks are seen in between the main peaks.

Small second peaks seen here do not describe the large peaks seen in several of the mosquito signals. Therefore, another projected area graph was done from a new orientation. This new orientation has the mosquito directly facing the direction that the laser beam is coming from. As there are numerous orientations possible, not many of them have been plotted yet.

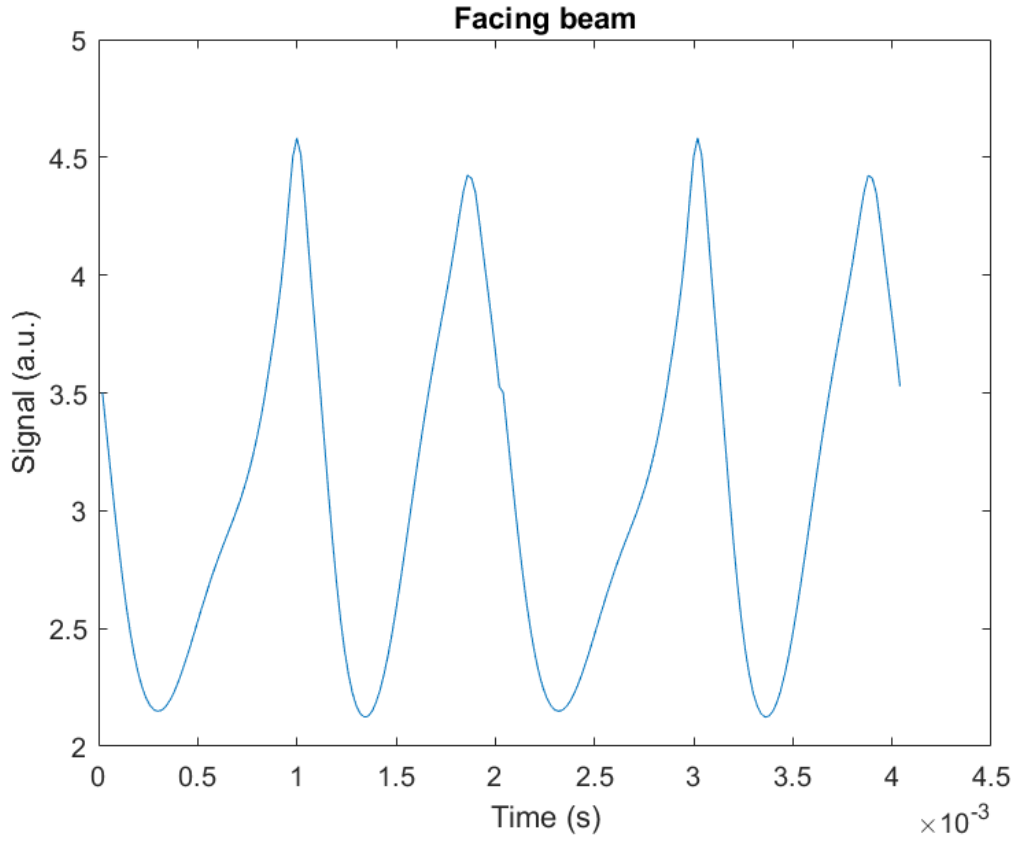

Figure 4.7 Projected area of a mosquito using a front view of a mosquito over two full cycles. Here, two peaks are seen over one cycle, with a very strong second peak visible.

If the previous theory is correct that the sharp peaks are caused by specular reflection of the wings, then this could introduce problems. The wing contribution in the signal is not necessary caused by the cross section of the wings, but by the angle that they face. Therefore, the ratio is not only surface area, but also strongly influenced by the orientation of the insect. If the amount by which specular reflection increases the signal is calculated, it could be possible to extrapolate the true wing beat surface area, and use this value instead.

One category often stated to be used in species characterization is the body to wing ratio. As mosquitos can be different sizes, it is possible that this value could be used for

identification. Comparing Tables 4.2 and 4.3, there is a clear difference in ratios that appear. However, there are two limitations that prevent this from clearly being able to be used for characterization. First of all, the standard deviation varies greatly in both species. As there are four broad categories, each includes a wide range in ratios. Further categories could further limit the range so that greater certainty is achieved. Secondly, the male *Aedes Albopictus* contains 103 mosquito events, while the male *Culex* Species only contains 25 events. Statistically, these numbers are far apart, with far less events in each category in the *Culex* species. As there is a large standard deviation in many of the ratios, the results could change with more samples.

In addition, the sharp/double category is one that can be expanded upon greatly. A large variety of peaks that appear differently appear here. In general, this category was reserved for sharp peaks, that appeared twice within one wing beat frequency, but the strength of the second peak ranged from barely visible but still distinguishable from the noise, to very close in strength to the regular wing beats. Expanding upon this range and differentiating the body to wing ratio between more categories of the double wing beat peak could lower the standard deviation that appears.

It is well known that female mosquitos that have recently fed are unable to fly very far. At one point, we received measurements from a mosquito that had recently fed on blood. However, there were not enough measurements made to draw a conclusion from. More signals than usual appeared to have dull wing beats, but there were not enough total signals to be statistically relevant.

In order to study how the wing beat of a single mosquito may vary, one particularly long signal was observed. This signal was approximately 0.53 seconds long, giving a

period of time where the mosquito's wing beat frequency was likely to change. In order to observe the wing beat frequency over individual wing beats, the peaks were used. The local maxima of each peak was considered the wing beat, and from two maxima, a frequency was calculated without using the Fourier transformation. Over the entire length of the mosquito event, there are multiple regions where the peak is not clear, and therefore a frequency is not measured there. In Figure 4.8, this is signified by a change in color to the graph.

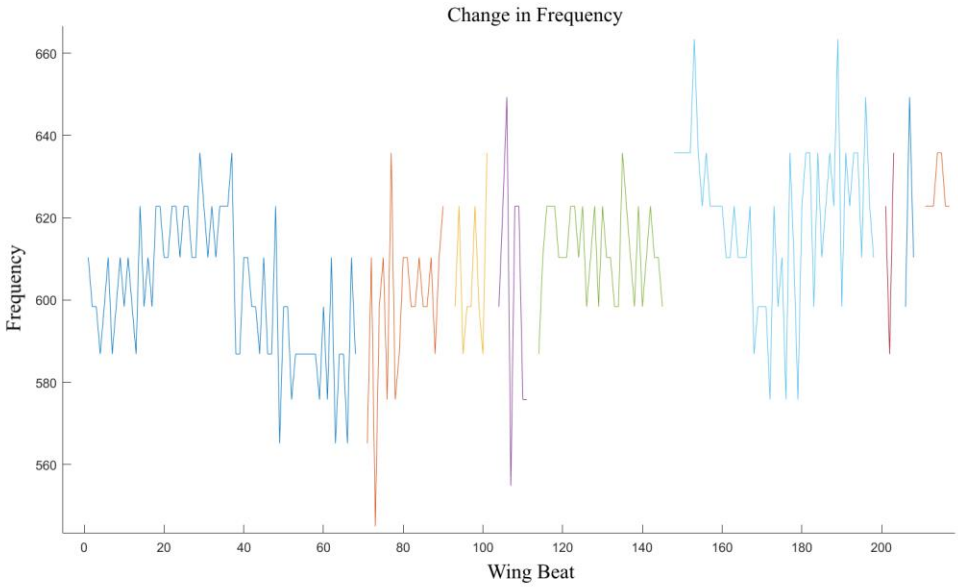

Figure 4.8 Change in Frequency over a large time period. The x-axis is every wing beat that is measured.

In a span of half a second, the frequency of the mosquito varies greatly. Excluding the extreme changes in frequency that occur the frequency varies from 565 to 635 Hz. Although some of the extreme changes in wing beat frequency can be explained by the peak in the signal not measuring a frequency precisely, there is still a noticeable trend where the mosquito will change frequency. Overall, there appears to be an upward trend with frequency growing higher.

In addition to the two species of mosquitos that were obtained, two other insects were captured and measured using the laboratory set up. This was done to see how different insects would appear in the signal and whether they would be easily differentiated from the mosquitos. The two insects were a common housefly, or *Musca domestica,* and a drain fly, of the family *Psychodidae.* Both of these insects were identified by eye, and measured using the same set up and specifications as the mosquitos. Their wing beat frequency results are listed in Figure 4.11.

One additional possibility of classification between sexes of mosquito species could come from their transit time. The average transit time in signals for the male *Aedes Albopictus* and *Culex* mosquito was 0.135 seconds and 0.145 seconds respectively, while it was 0.065 seconds and 0.069 seconds for the female of the same mosquito species. This may be a result of a different flight speed of each, although no literature has been found that suggests this. For now, more tests must be run for a more conclusive theory.

4.3 Comparison to Simulation

In order to calibrate the simulation to ensure accuracy, several values had to be adjusted. Once these changes were made, the results of the simulation were accurate compared to that of the experiments. Comparing Figure 3.3 to Figure 4.2 shows both similarities and differences. The most obvious arises from the wing beat peaks. As previously mentioned, a majority of the wing beat peaks present were sharp peaks that are believed to occur when there is specular reflection. This, alongside with the fact that the wing beats did not appear to be sinusoidal in signals, make the wing beats appear different. Specular reflection increases the recorded signal greatly, possibly accounting for the

different in signal strength. The simulation assumed entirely Lambertian reflection, where in an experimental setting, more backscatter occurred at the 180 degree angle. In one recorded signal, the SNR reached up to 33.9 compared to the 11.2 of the simulation. This is a factor of three.

Therefore, it is safe to assume that a larger distance than expected would be possible from the outdoor set up in the simulation. Although obtaining a SNR of 10 at 30 meters, as previously assumed, would result in a large distance being possible, this new information would mean that further distances are possible. Mosquitos fly at low heights, so if a drone were to be outfitted with this LIDAR system, it would be possible to point at the ground and obtain good results. If placed on the ground, we can assume that more than 30 meters could result in a good signal.

Another noticeable difference is the time period of which the mosquito is visible in the signal. In the simulation, although the mosquito is assumed to fly well below its maximum speed, it appears to fly even slower experimentally. This causes the time period which the mosquito is present in the laser beam to be longer.

Different body and wing contributions also appear in signals such as Figure 4.2. For a short period of time, the wings are visible as sharp peaks before the body contribution is even seen. This occurs as the mosquito may have their wings only in the laser beam as they extend further than their bodies. Erratic flight behavior of the mosquitos also appears as uneven signals, which alongside the orientation possibilities, account for many of the differences seen between simulation and experiment.

Apart from differences in the structure of the signal, there are sources of error in the values input in the equations. The reflection of the mosquito's body and wings is

estimated at 40%, but sources vary, including Figure 2.1, which put absorbance at 50%. A margin of error could come from the measurement of the cross section of the body, which was mostly done by eye, in addition to the difference in male and female mosquito size.

A large source of error comes from the beam spatial profile. The laser beam spatial profile has not been measured, which makes it difficult to implement into the numerical simulation. The Gaussian function is an approximation for the beam spatial profile.

As stated previously, there is a shadow caused by the sending mirror and post in front of the parabolic mirror which reduces the signal it receives. As shadow is difficult to measure, the value used is estimated.

4.4 Data Analysis

An important aspect of any experiment is how the data is analyzed. In order to locate when the mosquitos had passed the beam in a set of data that is lengthy (> 1 minute), a MATLAB program was created which would be used to find the areas where a mosquito likely crossed the laser beam. It also calculated the wing beat frequency of the mosquito. What was considered the wing beat frequency of the insect is the peak, or highest point, of the Fourier transform of the data, and not the middle of the full width half max. Only the range of 380:800 of the Fourier transform was considered. The following is the process used to find possible mosquito sightings.

t is defined as the total time in seconds of recording and Fs as the sampling frequency used. The following was done to filter and find the appropriate mosquito sightings:

1. The time, t, is split into one second intervals. The Fourier transformation is taken of each second into Fs number of bins.

2. The peaks and width using the findpeaks function are observed in the range between 380 and 850 Hz, the likely frequencies of the mosquito wing beat. These values are adjusted according to the species of mosquito used.

3. If the peaks are sufficiently high and widths sufficiently wide (of the findpeaks function), then that time period most likely has a mosquito sighting in it.

4. A few more filters are placed in order to lower the sensitivity to random signals or noise. For example, the signal must have values above the baseline noise and cannot have such a large range or value that it is not an insect. This prevents saturated signals from being interpreted as a mosquito sighting.

The wing to body ratio was calculated by a program as well. Using the wing beat frequency as a unit of time, a window was created which contained a signal wing beat. p is used as the number of wing beats to observe for this calculation. An odd value is used so that an even amount of wing beats on each side, starting from the center, maximum wing beat. An experimental program is being tested that will count every wing beat that appears over the entire signal, but it has not been finished.

1. Finding the index of the maximum point of the wing beats. This method operated on the assumption that there were multiple wing beats surrounding this maximum.

2. Depending on the width of the frequency bin findpeaks function, the number of points, p, are chosen. A higher width would likely mean that more wing beats were visible and a larger p value could be chosen, while a lower width would likely mean the opposite.

3. A window the size of one wing beat is made, using the Fs and the wing beat frequency found. This window is shifted to the left p/2-1 over to begin left of the maximum point.

4. At each window, a minimum and maximum value is found, where the wing contribution is at its highest and lowest. The highest contribution assumes that the wing is fully seen, while the lowest contribution assumes that there is no wing contribution and only the body of the mosquito is contributing to the signal. This window slides down, measuring multiple wing beats.

5. A noise reference is taken over the entire one second window where the mosquito sighting is. This noise reference is the mode of that window. The minimum value in a window minus the noise reference is considered the body contribution, while

the maximum value minus the minimum value is considered the wing contribution. An average is taken from all the windows.

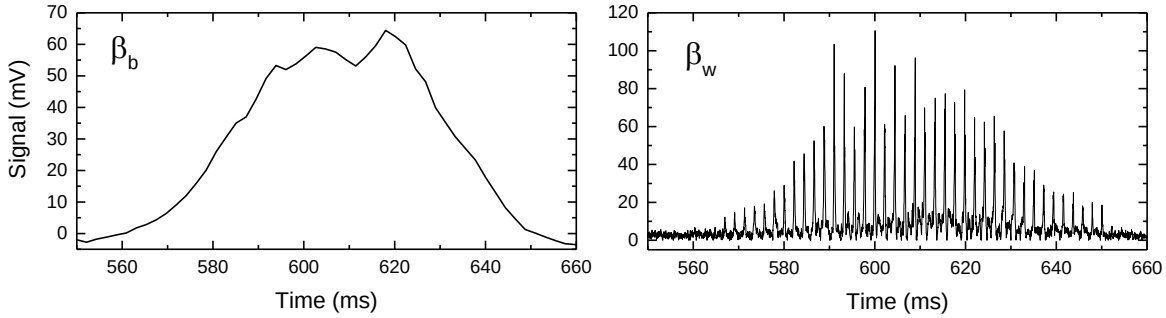

Figure 4.9 Separation into body and wing contribution. See Figure 4.2 for original signal. The MATLAB program returns a body to wing ratio of 0.94628.

There is a wide distribution of body to wing contributions that appear here. This is believed to be because of small movements of the mosquito, and changes in its orientation. Additionally, closer to the center of the laser beam, the laser beam spatial profile is stronger.

A minimum of 26 usable measurements existed for each individual sex and species of mosquito. Each of these signals had their wing beat frequencies recorded, then all signals from one sex and species were fit with a Gaussian distribution.

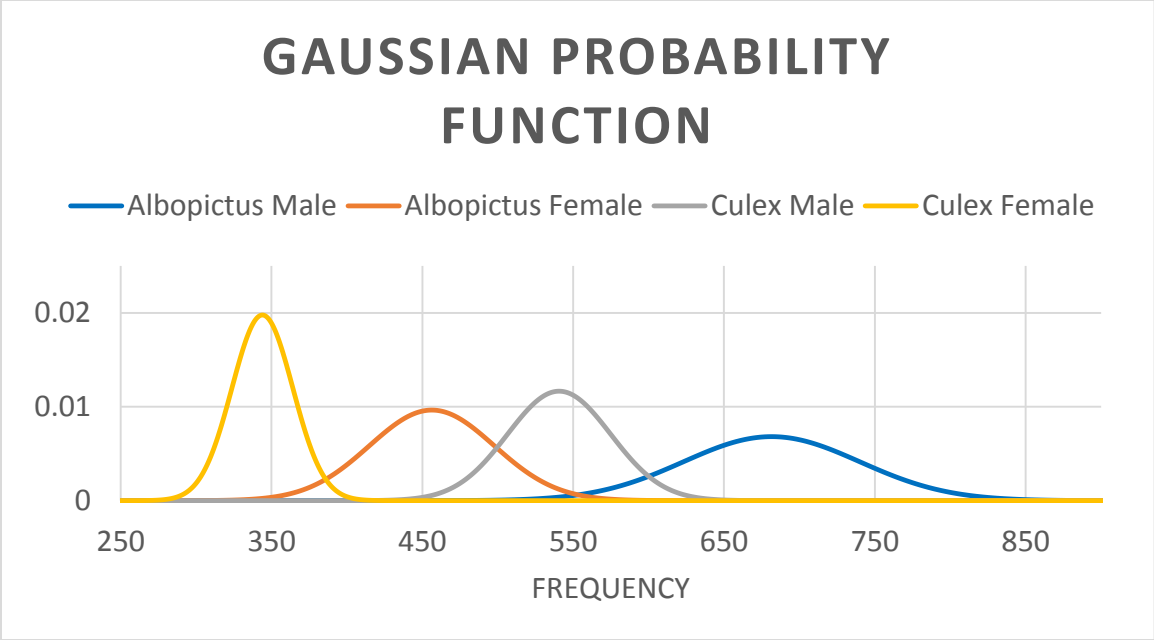

Figure 4.10 Gaussian fit over mosquito frequencies. All of the frequency data points of the mosquitos have been plotted on a Gaussian fit. While there is a bit of overlap between the female *Albopictus* and male *Culex*, they are still distinguishable for the most part.

The frequencies between the insects tested are different enough that they can be distinguished. Using a single species, the frequency ranges are far apart that a male and female can be distinguished with ease. Between the two species, the frequencies are still far apart that some characterization can be done based on the wing beat frequency.

The female Aedes Albopictus and male Culex had the only significant overlap in wing beat frequency. Other sexes and species tested could be differentiated by frequency. This gives credence to the theory that LIDAR could be used for the characterization of mosquitos. In addition to frequency, the body to wing ratio seems to be useful in characterization if the orientation of the insect is known. This additional characterization allows for more accuracy in insect classification.

Some interesting results stem from the width of each Gaussian function. The male *Aedes Albopictus* mosquito had a wide Gaussian fit, as this had a wide range of frequencies

measured, while the female *Culex* mosquito had a much taller fit, because of a lower range of frequencies.

With additional mosquito species, more data could be added to compare the wing beat frequencies across multiple species. In a field setting, multiple signals would be required to establish classification of one population. In addition to mosquito, two other insects were recorded, and had their frequencies fit with Gaussian distributions.

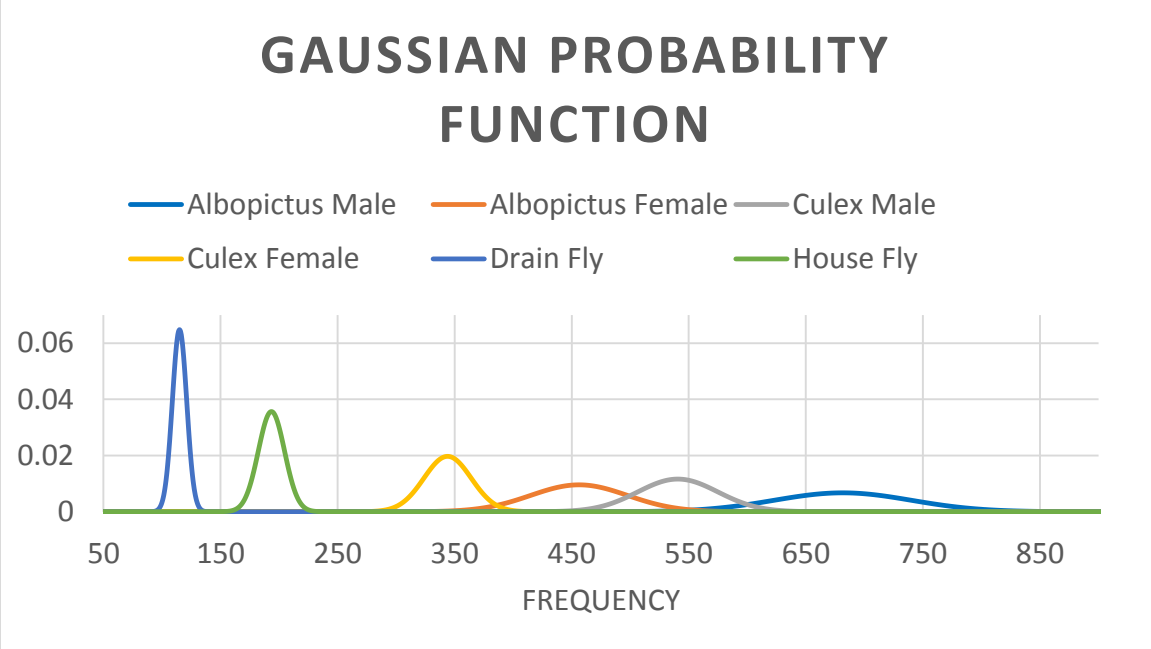

Figure 4.11 Gaussian fit over all insects. The two flies measured are different enough that differentiating between mosquitos and these two flies is possible with only the wing beat frequency.

The house fly and drain fly wing beat frequency results are much lower than the mosquitos, which means mosquitos should be easily characterized, at least compared to the larger insects tested here. Obviously this is not an absolute indicator that mosquitos will be distinguishable, but these two fly species are a good start in allowing this system to classify different insects. A clear difference can be seen between two distinct types of insects.

CHAPTER 5

CONCLUSION

5.1 Discussion

In this report, a new methodology was assessed that remotely monitored flying mosquitos using an infrared LIDAR system. The numerical simulation was used to study the feasibility of this new method. Important values such as the signal to noise ratio as a function of distance were retrieved, which shows that in an outdoor setting using the same equipment, a distance up to 45 meters can be recorded. A laboratory set up was also made and optimized which was an effective proof of concept. Both the body to wing ratio and the wing beat frequency can be determined. Between the two species of mosquito tested, the two sexes can be easily differentiated, which is promising for future classification. However, as the wing beat frequencies do overlap slightly, there is a slight degree of error.

Additional information can be obtained about the flight pattern of the mosquito by observing the wing beat peaks and the body to wing ratio. However, for additional characterization, and to ensure a higher degree of certainty about species classification, more characterization should be added.

While about two signals were usually obtained every minute, this was done in an enclosed container with minimum air flow and limited space. The mosquitos did not appear to move normally on the plastic tube as much as they did in their paper container, possibly limiting their frequency they were in flight. If an enclosure that more closely resembled their natural habitat was used, it could be possible to obtain signals more often.

5.2 Future Direction

5.2.1 Dual Wavelength

While the body to wing ratio and wing beat frequency will give some information about the insects that fly through the beam, they may not tell the full story. Both of these values are not constant for mosquito species, even for the very same mosquito. As orientation, speed and direction of flight can vary, these values will appear different every time. Additionally, some families of insects such as *Psychodidae* (drain fly) and smaller *Chironomidae* (lake fly / nonbiting midge) insects have wing to body ratios that overlap with that of mosquitos. Similarly, multiple other insects have wing beat frequencies that vary between 100 Hz and 1000 Hz. This overlap and variance among insects mean that there must be additional characteristics and approaches to differentiate mosquitos apart if high accuracy is desired, to allow more species of mosquitos to be characterized.

Two wavelengths will be used in the future parts of the project. Currently, only a 1.32 μm (Infrared) laser is being used. Reflectance is dependent on wavelength, and will change as the wavelength does. 1.32 μm was chosen as it had a high value of reflectance. A 950 nm laser is being considered here as it still has a high reflectivity for insects. It is the future goal of this project to have the ratio of the signal between each wavelength aid in characterizing and identifying insects.

5.2.2 Polarization

Light is known to be a wave, which can vibrate in multiple directions and planes. Polarizing light means to filter out certain directions of vibration so that only one plane of vibration passes through. Applying the knowledge of polarization to this system, information can be gained about the surface that light has interacted with. In the case of the mosquito,

polarization can be used to tell how smooth the surface of the mosquito is. As mosquitos can range from smooth, segmented and covered in small hairs, this information can be of use to further characterize signals received back from the LIDAR system.

The signal from both wavelengths mentioned in the previous section will be split and one of the reflected laser beams will be polarized in two planes. The ratio between the two planes of polarization can be observed and studied. For example, the male *Aedes Albopictus* mosquito has fuzzy antenna, while the female *Aedes Albopictus* has smooth antenna. If this feature is visible, it adds criteria to base classifications upon. Alongside the wing beat frequency, these details allow more certainty with classification. These two additions to the LIDAR system will allow for far more characterization to be done to more insects, and will give further information in their classification.

APPENDIX A

PHOTODETECTOR SETTINGS AND SPECIFICATIONS

The 50 gain step is used in Section 4 throughout as a high bandwidth is not necessary. In future experiments, a 0 or 10 gain step might be utilized.

Table A.1 InGaAs Transimpedance Amplified Photodetector (PDA20CS) gain setting chart.

Gain Step (dB)	Gain (+/- 2%)	NEP (pW/sqrt(Hz))	Bandwidth (Hz)
0	0.75 kV/A	51.2	10,000,000
10	2.38 kV/A	31.1	4,000,000
20	7.5 kV/A	6.54	1,870,000
30	23.8 KV/A	3.04	660,000
40	75 kV/A	1.14	200,000
50	238 kV/A	2.91	67,000
60	750 kV/A	1.76	25,000
70	2.38 MV/A	5.89	4,000

APPENDIX B

LASER SPECIFICATIONS

Laser power vs. Current. Although the laser came with this chart, tests were ran to ensure accuracy.

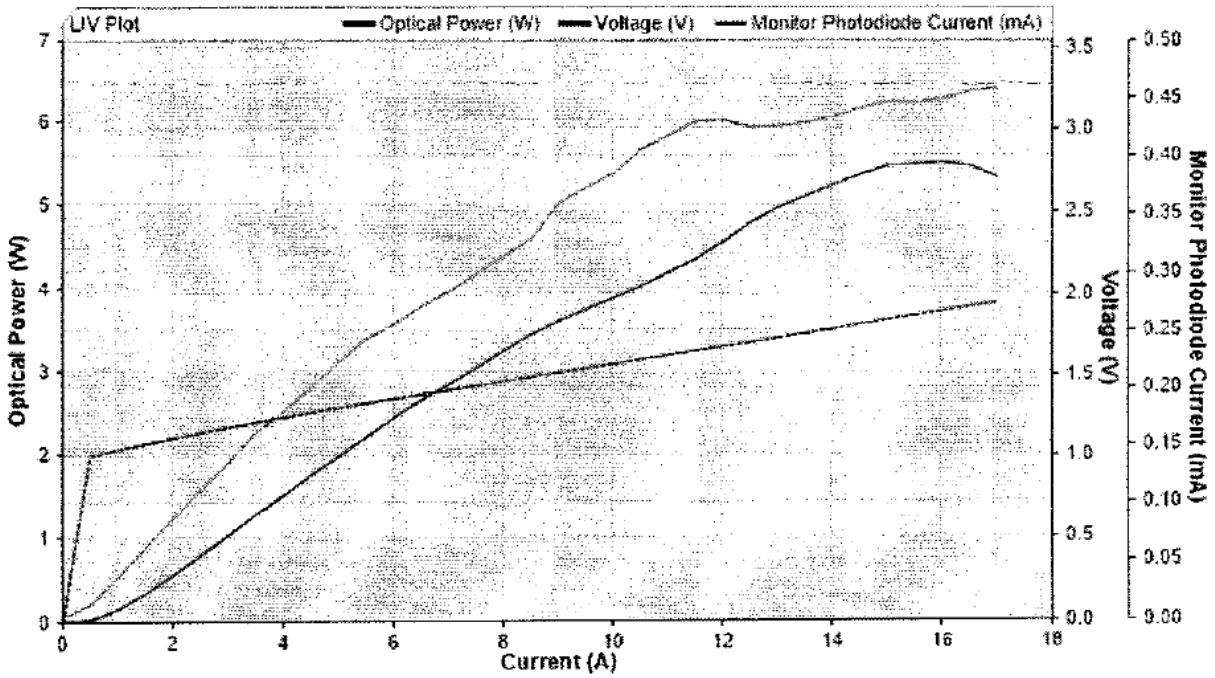

Figure B.1 Output of laser according to current input. Used in addition to calibration measurements to determine optical power.

APPENDIX C

NUMERICAL SIMULATION SOURCE CODE

The MATLAB source code that describes the numerical simulation that is used.

```
%          Christo Videlov          %
%  LIDAR Mosquito Detection Simulation  %
%              8/1/17              %

prompt= {'What distance is the mosquito? (meters)',...
   'What is the average value of the noise? (Microvolts)' ,...
   'What is the standard deviation of the noise? (microvolts)',...
   'What is the modulation frequency of the signal? (Hz)' ,...
   'What is the wing beat frequency of the insect? (Hz)',...
   'Is the mosquito in the beam perpendicular or sideways? (P/S)',...
   'Would you like a plot of the signal? Y/N '...
   'Which gain step would you like to use? (0-70, increments of 10)'};
dlg_title = 'User Inputs';
num_lines=1;
defaultans= {'3.6' ,'1880','476.7', '0', '600', 'P', 'Y', '50'};
UserInput=inputdlg(prompt,dlg_title, num_lines, defaultans);
% Allows the user to input multiple variables in the simulation

d=str2double(cell2mat(UserInput(1))); % Distance
avgnoise=str2double(cell2mat(UserInput(2))); % Average noise
stdnoise=str2double(cell2mat(UserInput(3))); % Standard deviation of noise
mfreq=str2double(cell2mat(UserInput(4))); % Frequency that signal is modulated
wingbeat=str2double(cell2mat(UserInput(5))); % Mosquito wing beat frequency
dirofins=UserInput(6); % Orientation of insect
dirofins=char(dirofins);
gainstep=str2double(cell2mat(UserInput(8))); % Gain step
% Converts these variables from cells to their formats (doubles/characters)

c=299792458; % Speed of light m/s
adj=(2*d)/c; % Time shift from distance
r=0.0127; % half an inch (in meters), initial radius of the beam
div=(1*10^-3); % Divergence of beam over distance
time=((r+(d*div))/0.67056); % Time mosquito is in beam from distance
... Multiplied by 4 to closer match real signal

if(gainstep == 0)
t=linspace(0-adj,1-adj,10000000); % Time initialize function, 1 second, 10 MHz
resolution
```

```
elseif (gainstep == 10)
t=linspace(0-adj,1-adj,4000000); % 4 MHz resolution
elseif (gainstep == 20)
t=linspace(0-adj,1-adj,1870000); % 1.87 MHz resolution
elseif (gainstep == 30)
t=linspace(0-adj,1-adj,660000); % 660 kHz resolution
elseif (gainstep == 40)
t=linspace(0-adj,1-adj,200000); % 200 kHz resolution
elseif (gainstep == 50)
t=linspace(0-adj,1-adj,67000); % 67 kHz resolution
elseif (gainstep == 60)
t=linspace(0-adj,1-adj,25000); % 25 kHz
elseif (gainstep == 70)
t=linspace(0-adj,1-adj,4000); % 4 kHz
else
   displacement('This is not a valid gain step');
end;
% Time resolution according to gainstep specified
hz=length(t);

amp = 0.1428; % Amplitude of modulation signal
% 0.2304 = 2.5 - 4 Watts
% 0.1428 = 3 - 4 Watts
% 0.0955 = 3.3 - 5 Watts
% (1/15) = 3.5 - 4 Watts
% 0.0525 = 3.6 - 4 Watts1
% 0.02562 = 3.8 - 4 Watts

% Power which it is modulated about
% I = 3.25; % 2.5 - 4 Watts
% I = 3.65; % 3.4 - 4 Watts
% I = 3.9; % 3.8 - 4 Watts
% I = 3.8; % 3.6 - 4 Watts
% I = 3.75; % 3.5 - 4 Watts
% I = 3.5; % 3 - 4 Watts
%Io = I*(1+amp* cos(2*pi*t*mfreq)); % initial signal with frequency
I=3.75;

displacement=0.0002*length(t); % Time for insect to fully enter/exit beam
ta=linspace(0,0.5,length(t)/2); % First part of time resolution
tb=linspace(0.5,1,length(t)/2); % Second part of time resolution
timetopoint=time*(length(t)); % time insect is in the beam converted to index
timetopoint=round(timetopoint); % Rounded to nearest number
timetoa=((length(t)/2)+timetopoint); %Body begins to leave beam
timetob=((length(t)/2)+displacement+timetopoint);%Body totally leaves beam
timetob=round(timetob); % Rounded to nearest number
```

```
if (timetob>length(t))
   disp('You have input too long a distance, and therefore too long a time.');
else
end;
% prevent times which are too long
u=.50+time/2;
%omega=time/3.229;
omega=time/5;
%G=(1/(omega*sqrt(2*pi)))*exp(-.5*(t-u/omega).^2);
G=(1/(omega*sqrt(2*pi)))*exp((-(t-u).^2)/(2*omega.^2));
G=G/82.0597;
msize=0.0026; % Mosquito body cross section
csbody=-16.5*t+(16.50652*(timetoa/length(t))); % Slope for mosquito body leaving
csbody(timetob:length(t))=0; % No mosquito
csbody(1:(length(t)/2))=16.5.*ta-8.2467; % Slope for mosquito body entering
csbody(1:round((length(t)/2)-displacement))=0; %  No mosquito
csbody((length(t)/2):timetoa)=msize; % Maximum mosquito body in beam
% Simulates mosquito entering beam. Time is according to distance and
... size of the beam. It has a linear slope for the mosquito to enter and exit
if (gainstep == 50)
csbody(67000)=0;
end;
%Fixes an error with 67 kHz bandwidth where last index is a large number

wing=0.0008*2; % Cross section of wing, there are two
if (dirofins=='P'|| dirofins=='p');
cswing=wing*sin((t*2*wingbeat*pi))+wing; % Wing beat simulation, frequency of 600
elseif (dirofins == 'S'|| dirofins == 's');
cswing=(wing/2)*sin((t*4*wingbeat*pi)+pi)+wing/2; % Sideways, twice the frequency
...half the amplitude
   else
      disp('Not a valid orientation of insect.')
end;
   cswing(1:round(length(t)/2-displacement))=0;
   cswing(round(timetoa+displacement/2):length(t))=0; % No mosquito

cswing(1:10)=0; % No mosquito
cswing((timetob+1000):(size(t)))=0; % After mosquito leaves
bbody=0.4; % Backscatter of body
bwing=0.4; % Backscatter of wing
% Values range from 20% to 60%, middle value chosen

% This is the original signal, used for phase shift measurements
% It=I*(1+amp* cos(2*pi*mfreq*(t-adj))); % Initial signal, that accounts for time shift in
signal
```

```
%It(1:10)=0;
% It is used only in the Iphase to account for the distance traveled

mirrorsize=0.0206; % Size of parabolic mirror
K=(mirrorsize^2)/(2); % formula for the surface of the parabolic mirror.
%K=(mirrorsize^2/2*d^2);
% .0254 is the laboratory setup (1 inch radius)
% .254 is the outdoor setup (10 inch radius)
% 0.0206 corrected for shadow

% PofI=((msize*100)+(wing*100))/(pi*(r*100)^2); % Percentage of beam spatial profile
reflected back
%SpatialProf=cos((236)*t);% Parabolic beam spatial profile
%60 When multipled by 4
% 236 when normal time
Id=0.85*0.97^3*(K/d.^2).*I.*G.*(((csbody*10^-3).*bbody+(cswing*10^-
3).*bwing)/(pi*(r+(div*d)).^2)); % Signal recieved,
...no modulation, used after distance is calculated 0.97 reflection of gold mirror

% Iphase=(K/d.^2).*Id.*(csbody*bbody+cswing*bwing)/(pi*(r+div.*d).^2); % Signal
recieved, modulation

baseline=0;
noise=(10^-6)*(avgnoise+stdnoise*randn(size(t))); % noise of detector
noise=noise*6;
% minnoise=-170micro
% maxnoise=3.87 mV
if (gainstep == 0)
Vx=(750); % total signal converted to volts, according to the listed gain of the detector
elseif (gainstep == 10)
Vx=(2.38*10^3);
elseif (gainstep == 20)
Vx=(7.5*10^3);
elseif (gainstep == 30)
Vx=(23.8*10^3);
elseif (gainstep == 40)
Vx=(75*10^3);
elseif (gainstep == 50)
Vx=(238*10^3);
elseif (gainstep == 60)
Vx=(750*10^3);
elseif (gainstep == 70)
Vx=(2380*10^3);
else
disp('Not a valid gain step');
stop
```

```
end; % How much the signal is multiplied by

V=Vx*Id+noise+baseline;
% Watts converted to Volts
% Noise multiplied by 6 for background

s=UserInput(7);
s=char(s);
if s==('Y');
   (plot(t,V));
else
end;
% Plots the voltage vs time if user specifies

%SNRV=(Id((hz/2):timetoa).*Vx); % Signal without noise/baseline
%SNRV=SNRV((length(t)/2)+500:timetoa-500); % Limits to higher part of mosquito
%SNRNoise=noise(1:length((hz/2):timetoa)); % Noise to use as reference
%SNR=snr(SNRV,SNRNoise);
% SNR given in decibels
% Signal to noise ratio based on rms of each
SNRV=max(Id*Vx)-mode(noise);
SNRnoise=std(noise);
SNR=SNRV/SNRnoise;

% PSsignal2=fft(V((length(t)/2):timetoa));
% PSinitial2=fft(Io((length(t)/2):timetoa));
% PSsignal=hilbert(V((length(t)/2):timetoa));
% PSinitial=hilbert(Io((length(t)/2):timetoa));
% Phase=angle(PSinitial/PSsignal);
% Phase2=angle(PSinitial2/PSsignal2);

% end
%Test of two different sides of Phase difference
% As phase calculations are dependent on bandwidth,

output=['Signal to Noise ratio (db)   ','Phase difference   ','Calculated Distance',...
   '    Input Distance'];
output2=['       ',num2str(SNR),        ];%          ', num2str(Phase),'          ',...
  %num2str(Phase2), '                ', num2str(d)];

disp(output);
disp(output2);
```

REFERENCES

1 Arthur, BJ, Emr KS, Wyttenbach RA, Hoy RR. "Mosquito (Aedes aegypti) flight tones: Frequency, harmonicity, spherical spreading, and phase relationships." *The Journal of the Acoustical Society of America* 135, no. 2 (2014): 933-41. doi:10.1121/1.4861233.

2 Bomphrey, RJ., Nakata T, Phillips N, Walker SM. "Smart wing rotation and trailing-edge vortices enable high frequency mosquito flight." *Nature* 544, no. 7648 (April 29, 2017): 92-95. doi:10.1038/nature21727.

3 Bosch T, Amann MC, Myllylä R, Rioux M. "Laser ranging: a critical review of usual techniques for distance measurement." *Optical Engineering* 40, no. 1 (2001): 10. doi:10.1117/1.1330700.

4 Brydegaard M, Gebru A, Svanberg S. "Super Resolution Laser Radar with Blinking Atmospheric Particles — Application to Interacting Flying Insects." *Progress In Electromagnetics Research* 147 (October 10, 2014): 141-51. doi:10.2528/pier14101001.

5 Brydegaard M, Merdasa A, Gebru A, Jayaweera H, Svanberg S. "Realistic Instrumentation Platform for Active and Passive Optical Remote Sensing." *Applied Spectroscopy* 70, no. 2 (January 2016): 372-85. doi:10.1177/0003702815620564.

6 Caraballo H, King K. Emergency Department Management Of Mosquito-Borne Illness: Malaria, Dengue, And West Nile Virus, Emergency Medicine Practice, 16, 5, 1-23 (2014).

7 Crepeau TN, Unlu I, Healy SP, Farajollahi A, Fonseca DM. Experiences with the large-scale operation of the Biogents Sentinel trap, J. Am. Mosq. Control Assoc., 29, 177–180 (2013).

8 Farajollahi A, Kesavaraju B, Price DC, Williams GM, S, Healy SP, Gaugler R, Nelder MP, Field efficacy of BG-Sentinel and industry-standard traps for Aedes albopictus (Diptera: Culicidae) and West Nile virus surveillance, J. Med. Entomol., 46, 919–925 (2009).

9 Fujii T, Fukuchi T, Laser Remote Sensing, CRC Press Ed., (2005).

10 GBD 2015 Disease and Injury Incidence and Prevalence, Collaborators, Global, regional, and national incidence, prevalence, and years lived with disability for 310 diseases and injuries, 1990-2015: a systematic analysis for the Global Burden of Disease Study 2015, Lancet (London, England), 388, 10053, 1545–1602 (2016).

11 GBD 2015 Mortality and Causes of Death, Collaborators, Global, regional, and national life expectancy, all-cause mortality, and cause-specific mortality for 249 causes of death, 1980-2015: a systematic analysis for the Global Burden of Disease Study 2015, Lancet (London, England), 388, 10053, 1545–1602 (2016).

12 G.E.A.P.A. Batista, H. Yuan, E. Keogh, A. Mafra-Neto, Towards Automatic Classification on Flying Insects Using Inexpensive Sensors, 10th International Conference on Machine Learning and Applications and Workshops (ICMLA), 364–369 (2011).

13 Gebru A, Brydegaard M, Rohwer E, Neethling P. "Probing insect backscatter cross-section and melanization using kHz optical remote detection system." *Remote Sensing and Modeling of Ecosystems for Sustainability* XIII (2016). doi:10.1117/12.2236010.5178875839001.

14 Gibson G, Warren B, Russell IJ. "Humming in Tune: Sex and Species Recognition by Mosquitoes on the Wing." *Journal of the Association for Research in Otolaryngology* 11, no. 4 (October 26, 2010): 527-40. doi:10.1007/s10162-010-0243-2.

15 Guan Z, Brydegaard M, Lundin P, Wellenreuther M, Runemark A, Svensson EI, Svanberg S. "Insect monitoring with fluorescence lidar techniques: field experiments." *Applied Optics* 49, no. 27 (September 16, 2010). doi:10.1364/ao.49.005133.

16 Harrington LC, Poulson RL. Considerations for accurate identification of adult Culex restuans (Diptera: Culicidae) in field studies, J. Med.Entomol., 45, 1–8 (2008).

17 Kawada H, Sumihisa H, Masahiro T. Comparative laboratory study on the reaction of Aedes aegypti and Aedes albopictus to different attractive cues in a mosquito trap, J. Med. Entomol., 44, 427-432 (2007).

18 Kirkeby C, Wellenreuther M, Brydegaard M. "Observations of movement dynamics of flying insects using high resolution lidar." *Scientific Reports* 6, no. 1 (July 04, 2016). doi:10.1038/srep29083.

19 Mayagaya VS, Michel K, Benedict MQ, Killeen GF, Wirtz RA, Ferguson HM, Dowell FE. "Non-destructive Determination of Age and Species of Anopheles gambiae s.l. Using Near-infrared Spectroscopy." *American Journal of Tropical Medicine and Hygiene* 81, no. 4 (2009): 622-30. doi:10.4269/ajtmh.2009.09-0192.

20 McMeniman CJ, Corfas RA, Matthews BJ, Ritchie SA, Vosshall LB, Multimodal integration of carbon dioxide and other sensory cues drives mosquito attraction to humans, Cell, 156, 1060–1071 (2014).

21 Meeraus WH, Armistead JS, Arias JR. Field comparison of novel and gold standard traps for collecting Aedes albopictus in Northern Virginia, J. Am. Mosq. Control Assoc., 24, 244–248 (2008).

22 Rochlin I, Ninivaggi DV, Hutchinson ML, Farajollahi A. Climate Change and Range Expansion of the Asian Tiger Mosquito (Aedes albopictus) in Northeastern USA: Implications for Public Health Practitioners, PLoS ONE, 8, e60874 (2013).

23 Snow WF. "Field estimates of the flight speed of some West African mosquitoes." *Annals of Tropical Medicine & Parasitology* 74, no. 2 (February 19, 1979): 239-42. doi:10.1080/00034983.1980.11687334.

24 Weitkamp C, Lidar, Range-Resolved Optical Remote Sensing of the Atmosphere, Springer Ed., Berlin, New-York (2005).

25 World Health Organization, World Malaria Report 2014, (2014).